UNIVERSITETET I BERGEN

Characterizing the Infectious Pattern of Viruses Infecting the Haptophyte *Emiliania huxleyi*

by

Marius Rydningen Saltvedt

Master's Thesis in Microbiology

2019

Department of Biological Sciences

Table of Contents

Acknowledgements

I would like to acknowledge Aquacosm (funding from the European Union's Horizon 2020 research and innovation program under grant agreement No 731065) and the – VIMS-Ehux project ('The Vardi Group' http://www.weizmann.ac.il/plants/vardi/home) for setting up the mesocosm experiment.

I must start off saying how grateful I am for the two amazing years I've had with all of the wonderful people in the marine microbiology group. I want to give a huge 'thank you' to my main supervisor Ruth-Anne Sandaa for all of her hard work with guiding me through my master and for the countless advices and directions she has given me, which I will be forever grateful for. I would like to thank my co-supervisor Janice Lawrence for all of her help in my experiments and for sharing so much valuable knowledge that has aided me throughout my thesis. My co-supervisors Selina Våge and Gunnar Bratbak have my gratitude for correcting and giving me great feedback on my thesis. I am also truly grateful for all the help I got from Hilde Stabell, as I would not have been able to complete my experiments if it had not been for her. I want to give Kyle Mayers my gratitude for initiating to great discussions, both scientifically and socially. I would also like to thank Flora Vincent (Vardi Group – Weissman Institute) for letting me use her flow cytometric data and saving me a lot of work in R by quality trimming all the Illumina sequences for me. At last, I am forever grateful for my partner Maria for all of her support and patience throughout my master.

Abbreviations and Important terms

Burst size – Number of virus particles produced from the lysis of a single infected cell

Competition specialist – A host cell with high nutrient uptake and growth rate, but with a fitness cost of having poor immunity against viral attack

Defense specialist – A host cell with high viral immunity, but with the fitness cost of having poor nutrient uptake and low growth rate

DGGE – Denaturing gradient gel electrophoresis, a technique used to separate DNA fragments

DOM – Dissolved organic matter

DNA – Deoxyribonucleic acid

EhV – Emiliania huxleyi virus, a coccolithovirus belonging to Phycodnaviridae

Emiliania huxleyi – a ubiquitous calcifying eukaryotic algae within Haptophyta

EV – Extracellular vesicle, a non-replicative exosome that can carry nucleic acids, proteins lipids, metabolites and even organelles. Can be used in intercellular communication and influence various physiological and pathological functions

FCM – Flow Cytometer, a tool that in this study were used to quantify host cells and stained virus particles.

Generalist virus – A virus with a broad host range

Kill the Winner – A mathematical model based on the concept that competitors deal with limited resources in two ways: competition or defense. The competition specialists (the winner) has high growth rate, but will be top-down controlled by virus and predators, allowing the slower growing defense specialists to coexist.

MCP – Major capsid protein encoded by the *mcp* gene used in the construction of the capsid in viruses

Microbial loop – describes trophic interactions and how the flow of nutrients are moved to higher trophic levels

MOI – Multiplicity of Infection, ratio of agents (e.g virus) to target (e.g. cell)

MPN – Most probable number, is a serial endpoint dilution assay used to quantify infectious virus particles

OTU – Operational taxonomic unit, is used when classifying groups of closely related individuals

PCR – Polymerase chain reaction, used to amplify a specific DNA sequence

Phycodnaviridae – A family of large double stranded DNA viruses infecting marine and freshwaters phytoplankton

Relative MOI-concentration - The concentration of virus particles added in the experiments, measured in percent of total culture volume and is both relative and specific to this study

SNP – Single nucleotide polymorphism, a substitution of a single nucleotide that occurs at a specific position in the genome

Specialist virus – A virus with a narrow host range

Viral shunt – A mechanism that disrupt the flow of nutrients to higher trophic levels due to viral lysis

VLP – Virus like particle, which is presumably a virus particle

Summary

Marine viruses play an important role in biodiversity, population abundance and biogeochemical cycling of elements in the environment. They exhibit a broad range of infectious patterns and it is of ecological interest to gain further knowledge about these complex systems. This study investigated infectious patterns by cross-infecting three strains of the ubiquitous coccolithophore *Emiliania huxleyi* (CCMP374, CCMP371 and B) with three Emiliania huxleyi virus strains (EhV-99B1, EhV-208 and EhV-86). The infectious- and total virus particles were monitored by most probable number (MPN) and flow cytometry (FCM), respectively. Our results presented variations in both infectious and total virus particle production when the three host strains were infected by virus strain EhV-99B1. The two other virus strains, EhV -208 and -86, were only able to propagate on one host strain (CCMP374), but induced a reduction in growth on the other two host strains (CCMP371 and B). EhV -208 and -86 were in this study defined as specialist viruses, however, they did not present any beneficial traits that exceeded the generalist virus EhV-99B1, suggesting the presence of other traits that allow them to persist. On the other hand, the host strains displayed killing the winner dynamics, but further investigations are necessary. Additionally, this study assessed how the three host strains responded to EhVs sampled during a mesocosm experiment, where an *E. huxleyi* bloom crashed by viral lysis. The same EhV genotype was observed throughout the bloom and was phylogenetically distinct from EhV -208 and -86, but despite this, presented equivalent infectious pattern. At last, we were able to confirm that the burst sizes diminished with increasing MOI, which ultimately led to the same number of virus particles, regardless of the initial MOI. We proposed viral enhanced extracellular vesicles (EVs), which are actively produced by infected cells, as the causative agent for both the reduced growth in resistant host cultures and the diminishing burst sizes with increasing MOIs.

1 Introduction

1.1 Marine Viruses

In the late 1980s scientists discovered that viruses were the most numerated biological entity in the marine environment, present in concentrations of ~ 10^6 to 10^9 per mL, usually exceeding their host communities by one order of magnitude (Bergh et al., 1989; Proctor and Fuhrman, 1990; Wommack and Colwell, 2000; Suttle, 2007). Further research revealed high numbers of viral particles being constantly produced (up to ~5×10^9 virus liter^{-1} h^{-1}), while rapidly being inactivated as a result of viral decay within a few hours to days (Bongiorni et al., 2005; Fuhrman, 1999; Heldal and Bratbak, 1991; Munn, 2011; Noble and Fuhrman, 1997; Suttle and Chen, 1992). Our understanding of their active role in marine microbial communities and how they influence several important biochemical and ecological processes has increased tremendously the past decades (Breitbart, 2012; Fuhrman, 1999; Jacquet et al., 2010; Short, 2012; Suttle, 2007, 2005; Wommack and Colwell, 2000).

In the microbial loop, dissolved organic matter (DOM) produced by photosynthetic organisms (primary producers) is utilized and remineralized by the activity of respiring heterotrophic bacteria and archaea. Through grazing and predation of both heterotrophs and phototrophs the nutrients will move up into higher trophic levels (Azam et al., 1983; Bratbak et al., 1994; Fenchel, 2008; Munn, 2011). Virus infection and lysis of primary producers and heterotrophic organisms acts as a short circuit that disrupt the flow of nutrients to higher trophic levels. It is termed the viral loop or viral shunt and the lysis causes the host cell to release its cellular components and content in which will dissolve into the surrounding environment. Much of these cellular fragments, dissolved substances and virions are kept in the upper levels of the ocean as they do not sink (unless they particulate by aggregation) and becomes a nutrient source for bacteria, which can rapidly recycle these substances (Bratbak et al., 1994; Brussaard et al., 1996a; Dimmock et al., 2016; Fuhrman, 1999; Gobler et al., 1997; Munn, 2011; Suttle, 2007; Wilhelm and Suttle, 1999). Several members in the microalgal community are bloom forming and viruses may have a significant role in their bloom demise, some being responsible for 12-100% of the net mortality (Bratbak et al., 1993; Jacquet et al., 2002). Thus, viruses directly control the abundance of microorganisms and indirectly the fluxes of energy, nutrients and organic matter.

1.2 Phycodnaviridae and their haptophyte hosts

Marine phytoplankton strongly impact the global nutrient cycles and contribute with ~50% of the global carbon fixation (Falkowski, 1994; Falkowski and Raven, 2007). Haptophyte algae, a dominant clade of marine phytoplankton, occupy 30-50% of the total chlorophyll *a* biomass in the oceans with both bloom and non-bloom forming representatives (Liu et al., 2009). Many of its members produces an external plate layer made of calcium carbonate called coccoliths. These calcifying haptophytes are called coccolithophores and are ubiquitous throughout the ocean (Brown and Yoder, 1994; Holligan and Groom, 1986; Winter and Siesser, 2006). The cosmopolitan single-celled coccolithophore *Emiliania huxleyi* (Figure 1) is the most abundant and a well-studied species among coccolithophores (Brown and Yoder, 1994; Tsuji and Yoshida, 2017). *E. huxleyi* is a significant contributor in respect to marine primary production, especially in terms of global carbon and sulfur cycles (Burkill et al., 2002; Westbroek et al., 1993). Immense coastal and mid-oceanic blooms at temperate and sub-temperate latitudes are formed by *E. huxleyi*, usually flourishing in nutrient depleted waters after reformation of stratified pycnocline ocean layers. Blooms of *E. huxleyi* can cover >100,000 km^2 and dense formations can be seen in satellite imagery due to its reflective white or turquoise color (Ackleson et al., 1988; Holligan et al., 1993; Tyrrell and Merico, 2004). Such blooms have in recent years shown to typically terminate due to the activity of marine viruses belonging in the phycodnaviridae family (Bratbak et al., 1996, 1993; Brussaard et al., 1996b; Castberg et al., 2001; Jacquet et al., 2002; Schroeder et al., 2003; Wilson et al., 2002).

Phycodnaviridae is a family of large (100 to ~560 kb) double stranded DNA viruses that infects microalgae and are found worldwide in both marine and freshwater environments (Van Etten et al., 2002; Wilson et al., 2011). Occasionally they are found in high concentrations and regularly affect the microbial composition, diversity and important biochemical cycles in the aquatic environment (Wilson et al., 2011, 2009). Phycodnaviridae consist of 6 genera which to date are Chlorovirus, Coccolithovirus, Phaeovirus, Prasinovirus, Raphidovirus and Prymnesiovirus (Wilson et al., 2011, 2009).

Figure 1. Scanning electron microscope image of Emiliania huxleyi superimposed on a MODIS satellite image of an E. huxleyi bloom in the Barents Sea from 27 July 2004. Satellite image courtesy of Jacques Descloitres, MODIS Land Rapid Response Team, NASA; Inset SEM photo by Steve Gschmeissner, Photo Researchers, Inc. Image file obtained from <https://wis-wander.weizmann.ac.il/earth-sciences/lab-ocean>.

The Coccolithoviruses within the phycodnaviridae isolated so far, only infects the calcifying and bloom forming coccolithophore *Emiliania huxleyi* and are named Emiliania huxleyi virus (EhV) after its host. EhV have shown to express an animal-like infection cycle by entering their host through either endocytosis or an envelope fusion mechanism (Mackinder et al., 2009). The viral capsid is degraded in the cytoplasm and its DNA is transported and replicated in the host nucleus. The viruses are formed with an icosahedral symmetry and acquiring an external lipid membrane (envelope) by budding through the host membrane (Mackinder et al., 2009). Their genome size ranges from 376 to 421 kb and have a physical size range of 170 to 220 nm (Schroeder et al., 2002; Wilson et al., 2011, 2009, 2005).

Research on Coccolithoviruses have made it clear that they are closely involved in controlling their host populations and are especially important contributors of the sudden crashes of extensive costal and mid oceanic blooms of *E. huxleyi* (Bratbak et al., 1993; Jacquet et al., 2002; Schroeder et al., 2003; Wilson et al., 2002). During the progression of bloom events, it has been detected variations of both virus and host diversity. Using the major capsid protein (*mcp*) as a marker gene, the EhV strain diversity is initially high, but decreases as the bloom progress (Martinez et al., 2007; Schroeder et al., 2003; Sorensen et al., 2009). A similar pattern is often seen for the host population, monitoring genes encoding the calcium-binding protein (GPA), where the diversity decreases during the bloom formation (Sorensen et al., 2009), but not always (Highfield et al., 2017). Not only do the EhV diversity appear locally in blooms, but analysis based on complete genome and DNA polymerases clusters isolated EhV into distinct sub-clades, based on geographical region and time of isolation (Allen et al., 2007; Schroeder et al., 2002; Wilson et al., 2009). It is however clear, EhV populations are naturally very dynamic (Highfield et al., 2017) and the community composition can change over relative short periods of time (Sorensen et al., 2009).

1.3 Coevolution of viruses

The diversity in the marine phytoplankton community is enormous (Lovejoy et al., 2006; Pommier et al., 2007; Thompson et al., 2005) and surprisingly there are species and strains that can naturally coexist while competing for the same limiting resources (Fuhrman, 1999; Fuhrman and Suttle, 1993; Liu et al., 2009). A key question addressed in Hutchinson's paradox is: how can the abundance of different phytoplankton species persist in the marine environment when they all have very similar ecological roles and compete for the same limiting nutrients (Hutchinson, 1961)? A popular hypothesis based on a mathematical model suggest the diversity is maintained by the presence of virus in which 'kill the winner' (KtW), where the 'winner' is considered the most active microorganism in the population and not necessarily the most abundant (Thingstad, 2000). The KtW model suggests there is a continuous coevolution between the virus and host in an evolutionary arms race, where there is a constant selection pressure for the host to develop resistance and for the virus to overcome this resistance (Figure 2). This model also take into account that development of resistance has a fitness cost (Winter et al., 2010). Such a cost of resistance (COR) or trade-off, can for instance be changes in membrane protein or polysaccharide receptors that make the

strain less competitive if these molecules are involved in nutrients uptake or metabolism (Bidle, 2016; Martiny et al., 2014; Munn, 2011). This provides the basis for why competition specialists (high growth rate, low resistance) and defense specialists (low growth rate, high resistance) can coexist and over evolutionary time develop into the diversity we find today (Sheldon and Verhulst, 1996; Thingstad et al., 2014).

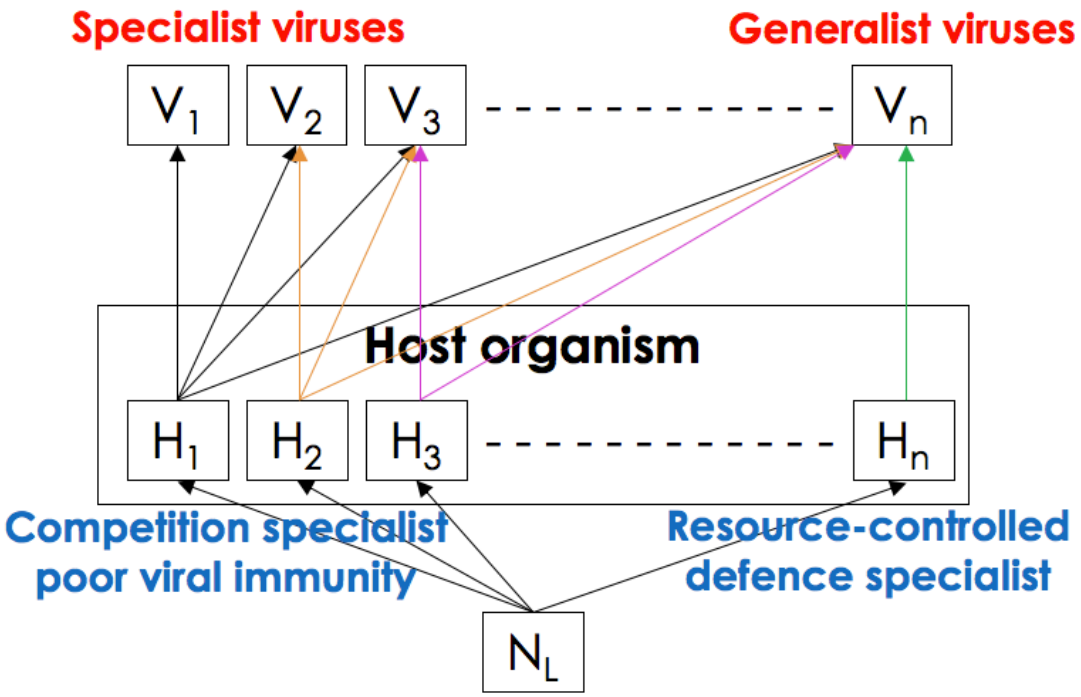

Figure 2. A simplified model from Thingstad et al. (2014) and Våge et al. (2016) representing a virus controlled host organism in a nutrient limited (N_L) system. Host strain H_1 is established early in the arms race and are specialized in competing for the limited nutrients (competition specialist), but its growth is suppressed by virus strain V_1. A resistant strain H_2 evolves from the parental strain H_1 due to viral selection pressure, but with a fitness cost of having lower growth rate. Mutants of V_1 gain an increasing host range (V_2 – V_n), being able to infect resistant strains, but with a fitness cost (e.g. infectious particle production, viral decay, absorption, burst sizes). The arms race between virus and host will lead to host H_n (evolved from ancient host strains) having high viral resistance capabilities (defence specialist), but with poor nutrient uptake. Early virus strains will have a narrow host range, termed specialists, while later evolved viruses with an accumulating host range are able to infect both ancient (H_1-H_3) and recently evolved host strains (H_n). Viral host range are indicated with arrows, where the host strains are separated by color.

For the viruses, the evolutionary arms race will lead to an accumulating increase in host range (generalists), while the ancient viruses will only have a narrow host range (specialists). However, for the specialist viruses to coexist and not be outcompeted by the generalist viruses, there should be a fitness cost of maintaining a broad host range (e.g. infectious

particle production, viral decay, absorption, burst sizes) that enables the coexistence of specialist and generalist viruses (Bidle, 2016; Martiny et al., 2014).

Metagenomic data has revealed an enormous virus diversity the last decade (Brum and Sullivan, 2015; Hurwitz and Sullivan, 2013; Paez-Espino et al., 2016) and strains of viruses has been documented to coexist in the same geographical regions (Cottrell and Suttle, 1991; Schroeder et al., 2002; Wilson et al., 2002), which support the KtW hypothesis. Good evidence for a KtW scenario is from blooms of phytoplankton such as *E. huxleyi* (Bratbak et al., 1993; Martinez et al., 2007) and *Heterosigma akasjiwo* or *Phaecystis globosa* (Nagasaki et al., 1994; Tarutani et al., 2000). High viral mediated mortality may cause the bloom to collapse (Bratbak et al., 1993), which can possibly produce greater diversity (Suttle, 2007).

A huge advantage with such diverse systems, which contain various levels of viral immunity and host specificity, is a possible regeneration of nutrients released by viral lysis (viral shunt), which in turn can become available for resistant or non-infected strains of the same species (Cottrell and Suttle, 1995; Munn, 2011; Suttle, 2007). Strain diversity will also make a species robust, where the faster growing strain will only be reduced in cell number, but not necessarily in total cell abundance of this species, assuming viral susceptibility varies between the strains (Brussaard, 2004; Fuhrman and Suttle, 1993; Wommack and Colwell, 2000). The viruses will thus not only control the host population size, but also the genetic and physiological diversity within the species from which the host can benefit (Hennes et al., 1995; Martiny et al., 2014; Middelboe et al., 2009; Tarutani et al., 2000).

1.4 Infectious patterns of algal viruses

Marine viruses exploit an enormous amount of different infectious patterns, varying in factors such as infectious units, viral particles, burst size, absorption efficiency, latency etc. (Bidle, 2016; Dimmock et al., 2016). One ecological important factor often overlooked in several studies is the number of infectious virus particles (titer), which is measured using plaque assays or a serial endpoint dilution assays (Most Probable Number, MPN). Studies have documented successful use of plaque assays for *Emiliania huxleyi*, *Micromonas pusilla,* cyanobacteria and *Chlorella* (Bratbak et al., 1996; Cottrell and Suttle, 1995; Van Etten et al., 1983a; Wilson et al., 1996) among others. However, as it is generally difficult to cultivate

pelagic phytoplankton species on solid media in plaque assays, it is most common to use the MPN method as the host cells can be cultivated in aqueous solutions (Brussaard, 2004).

The MPN method is not just limited to cultivated virus strains, it is also possible to estimate infectious particles from environmental samples. MPN-based studies of *Heterocapsa circularisquama* (Nagasaki et al., 2004), *Chaetoceros* sp. (Tomaru et al., 2011a), *Micromonas pusilla* (Cottrell and Suttle, 1995) or *Heterosigma akashiwo* (Tomaru et al., 2004) shows that number of infectious algal viruses typically ranges between 10^3-10^4 per mL in environmental samples. It is however important to keep in mind that MPN-assays are limited by the virus specificity in which is high in phytoplankton viruses and can possibly give lower estimates. An example is shown in Sahlsten (1998), where the highest number of infectious particles was obtained by using a host that was isolated close to the sampling area, which illustrates that the selected host strain might control the outcome (Short, 2012).

In addition to plaque assays and MPN techniques that provide numbers of infectious particles, flow cytometric or quantitative PCR tools can be used to estimate the total number of virus particles. From the infectious and total virus particle counts it is possible to calculate the proportion of infectious units in a viral population. It is ecologically relevant to investigate the number of infectious particles as it is often lower than the total particle abundance. The percentage of infectious particles to total particles can vary from just a few percent all the way to 100% (Bratbak et al., 1998; Cottrell and Suttle, 1995; Dimmock et al., 2016; Klasse, 2015; Suttle and Chan, 1993; Van Etten et al., 1983b).

The number of virus particles produced from lysis of a single infected cell are referred to as the burst size. For algal viruses it ranges from hundreds to tens of thousands of particles and viruses with smaller genomes typically have larger burst sizes compared to ones with larger genomes (Short, 2012). However, exceptions do occur, for instance between two diatom viruses that both have similarly sized circular single stranded DNA genomes (5600 and 5900 bp, respectively), where one infects *Chaetoceros lorenzianus* and has a burst size between 10^3 - 10^4 (Tomaru et al., 2011b), whereas the other infects *C. tenuissimus* and has an order of magnitude less burst size (Tomaru et al., 2011c). Considering the giant algal viruses (e.g. phycodnaviridae), which is classified as nucleocytoplasmic large DNA viruses (NCLDVs), typically ranges in burst size from 10^2 to 10^3 virus particles per cell (Short, 2012), but some

NCLDVs such as Chrysocromulina ericina virus 01B can release as much as 1800 to 4100 virus particles per cell (Sandaa et al., 2001).

Various environmental factors or even the growth condition of a host cell are known to affect viral burst sizes. For instance, a double stranded DNA virus, which infects the dinoflagellates *Heterocapsa circularisquama* changed in burst size from 1800 to 2440 particles per cell depending on if the incubation temperature were set at 20°C or 25°C, respectively (Nagasaki et al., 2003). *E. huxleyi* typically ranges in burst size between 400-1000 particles per cell (Bratbak et al., 1993; Brussaard et al., 1996a; Castberg et al., 2002; Dunigan et al., 2006), but decreases in burst size when the host culture is limited by phosphorous (Bratbak et al., 1993). A different study documented a change in burst size of infected *Phaeocystis pouchetii* culture depending on whether the host cells were in exponential or stationary phase (Bratbak et al., 1998).

It has also been reported that when *Aureococcus anophagefferens* cultures were infected with various multiplicities of infection (MOIs, ratio of virus to target cell), the burst sizes diminished with increasing MOIs (Brown and Bidle, 2014). In this study they proposed such a phenomenon to be caused by both lysis 'from within' and lysis 'from without', in which the cells lyse in two distinct ways (see below). This phenomenon was first described by Delbrück (1940) who noticed that the type of lysis in a bacterial-phage system was dependent on the initial MOI. At low MOIs (no higher ration than 2:1 of phages to bacteria) the phages seem to enter the cells, multiplied and lyse the cells 'from within'. However, when the MOIs where high (>100:1) the cells lysed directly 'from without' before any virus multiplication could occur, as a result of numerous attached phages weakening the cell wall. This is one of the many reasons why it is important to perform a one-step growth experiment to ensure that essentially every cell in the culture is infected and avoid large numbers of excess virus particles. It is of special importance when comparing the growth of two or more closely related viruses in order to possibly link differences in infectious pattern (Dimmock et al., 2016).

A recent study investigated the signaling role of extracellular vesicles (EVs) produced during viral infection in *E. huxleyi* (Schatz et al., 2017). EVs are non-replicative and are thought to be naturally released from most cells studied to date, including bacteria, archaea, protists, fungi, metazoans and plants (Brown et al., 2015; Kulp and Kuehn, 2010; Soler et al., 2008;

Szempruch et al., 2016). The EVs can for instance carry proteins, lipids and nucleic acids, that can be used for intercellular communication and possibly influence various physiological and pathological functions (Yáñez-Mó et al., 2015). Schatz et al. (2017) documented that EVs were highly produced during virus infection of *E. huxleyi* or when non-infected cells were exposed to infochemicals extracted from infected cells cultures. The EVs had a unique lipid composition compared that of virus particles and host, and carried small RNAs thought to be involved in sphingolipid metabolism and cell cycles. The absorption of EVs in host cells consequently lead to a more rapid infection cycle and also prolonged the half-life of the virus particles. The authors of this paper proposed that EVs may aid in faster terminations of *E. huxleyi* blooms (Figure 3).

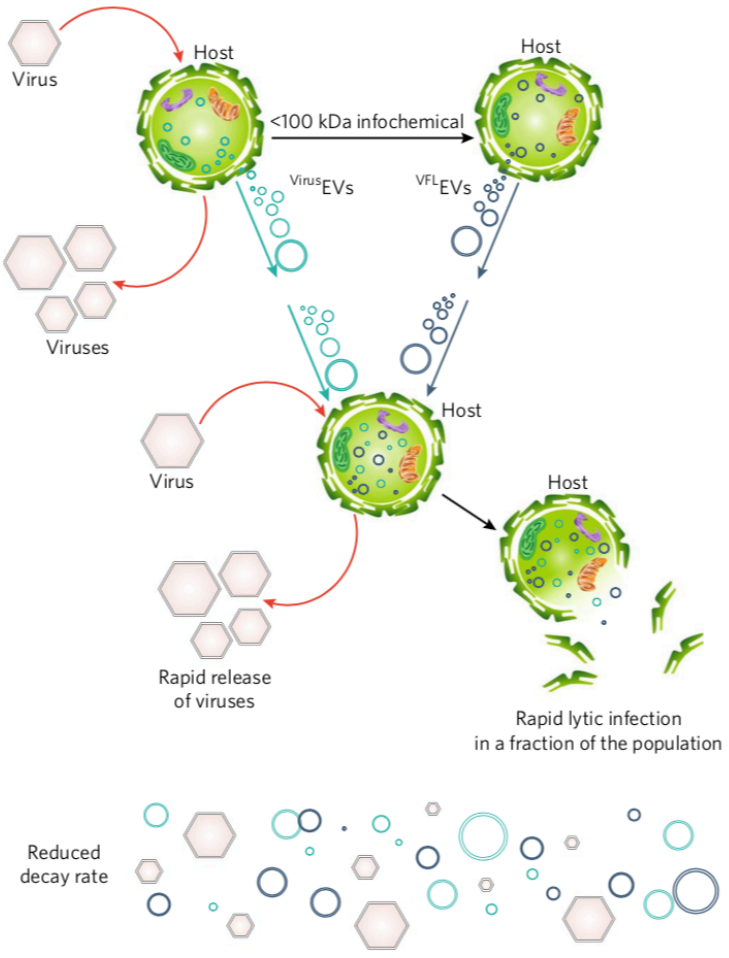

Figure 3. Proposed model to describe the effect of EVs on viral infection in the ocean obtained from Schatz et al. (2017). Infected *E. huxleyi* cells produce viruses, EVs and a <100 kDa virus-induced infochemical that induces EV production in naïve cells. EVs enter new cells, where they precondition the cells for subsequent viral infection that exhibits a faster lytic rate and higher viral production. Released EVs slow the decay rate of the EhV virions in the environment, which potentially increases the effective time for infectious encounters during *E. huxleyi* bloom dynamics.

Another interesting feature of viruses infecting *E. huxleyi* is that their genome contains an almost complete set of genes encoding sphingolipid biosynthesis pathway (SBP) that originates from the host genome (Wilson et al., 2005). Sphingolipids naturally act as signal molecules in the membrane of cells and can regulate processes such as cell cycle, differentiation or programmed cell death (PCD; Engelking, 2015). However, during infection there is an accumulation of viral encoded glycosphingolipids (veGSL) in the infected host cells, which triggers the release of virus particles (Vardi et al., 2009). Purified veGLS also seems to promote PCD in uninfected host cells, which is why the authors of this paper suggested that this is a mechanism that might increase the rate of viral termination of *E. huxleyi* blooms (Vardi et al., 2009).

The various and complex infectious strategies mentioned above, along with countless more, contribute to the idea that algal viruses have an enormous diversity in replication and infection strategies and that we have only surfaced what is out there. Marine viruses are important contributors in structuring the marine environment, which is why it is of ecological interest to investigate various aspects of their infectious patterns.

Project aims

The main objective of this master thesis was to investigate variations in infectious patterns between strains of *Emiliania huxleyi* and Emiliania huxleyi virus (EhV) based on virus particle and infectious production. We also wanted to investigate the infectious patterns using EhV from a mesocosm study in order to gain further understanding about strain specific virus-host interactions during bloom formations.

The following research questions were investigated:
- Are there significant variations in infectious patterns between virus and host at the strain level and does it reflect upon the virus having generalistic or specialistic properties?
- Will the infectious pattern vary between host strains when infected with EhV particles from a mesocosm study?
- To what extent is the viral burst sizes affected by MOI?

To answer these research questions, we first conducted a one-step growth experiment with various MOIs using three EhV strains on one *E. huxleyi* host strain. Secondly, we used the lowest MOI that maintained a one-step growth curve for each of the three EhV strains to separately cross-infect three *E. huxleyi* host strains. At last, we measured the number of infectious particles in a mesocosm using the same three host strain along with measuring the viral diversity.

2 Materials and Methods

Two studies were conducted in this master thesis, a cross-infection experiment and a mesocosm experiment. In the cross-infection experiment the main goal was to observe differences in infectious patterns between three *Emiliania huxleyi* host strains (CCMP374, CCMP371 and B) and three Emiliania huxleyi virus (EhV) strains in a one-step growth curve, where the production of infectious virus particles (MPN) and the total yield of virus like particles (VLPs) were compared. In the mesocosm experiment the main goal was to observe how EhVs from a natural community affected the three host strains, along with investigating the viral diversity during the bloom and determine the viral winner(s). These two experiments were compared to see if cultured virus strains displayed similar infectious patterns to viruses from a natural community.

2.1 Host and virus

2.1.1 Emiliania huxleyi strains

Three *Emiliania huxleyi* strains were used in this master thesis, CCMP374, CCMP371 and B. These strains were obtained from Bigelow Laboratory for Ocean Sciences, USA; and the University of Bergen, Norway (Appendix A, Table A-1). Strain CCMP371 and B were maintained in 50-600mL Erlenmeyer flasks with IMR/2 media (Appendix B.1, Table B-1), while strain CCMP374 was maintained with f/2 (Appendix B.1, Table B-2). All cultures were incubated in 16°C with a 14:10 h light:dark illumination cycle at ~50 µmol photons m^{-2} s^{-1} (Biospherical Instruments Inc. QSL-100, San Diego, California, USA) white light from fluorescent tubes.

2.1.2 Emiliania huxleyi Virus (EhV) strains

The three EhV strains used, EhV-99B1, EhV-208 and EhV-86, were obtained from the Plymouth Marine Laboratory, UK; and from the University of Bergen, Norway (Appendix A, Table A-2). These virus strains were propagated on exponentially growing *E. huxleyi* CCMP374 strain over several rounds of infection (>7), incubated at either 72- or 96h. Prior to new round of infection, the viral lysates were centrifuged at 5500 rpm for 15 minutes at 10°C (Beckman Coulter™, Allegra™ 2IR Centrifuge S4180 rotor, USA) in order to remove

bacteria and cell debris. The supernatant was transferred to a 50mL falcon tube and stored at 4°C in the dark until cultures were setup.

A 30mL exponentially growing host culture was infected with 3mL centrifuged viral lysate, 10% of the culture volume (total volume of 33mL). A control was maintained for each viral culture, prepared in the same way as the virus culture, except the lysate was replaced with 3mL media. The infected cultures containing the EhV strains, were consequently incubated for 72h prior to any experiment.

2.2 Cross-infection experiment

This experiment was divided in two, where the first part was to define the minimum multiplicity of infection (MOI, ratio of virus to host cells) needed to maintain a one-step growth curve for each of the three virus strains using CCMP374 as host (Figure 4). In the second part the three virus strains were cross-infected with the three host strains, infecting them with the minimum MOI that was obtained in the first part (Figure 5).

2.2.1 Defining the *minimum MOI that maintains a one-step growth curve*

A 600mL culture of *E. huxleyi* CCMP374 was prepared and diluted to ~5 x 10^5 cells/mL by estimating its cell concentration using counting chamber (Bürker, Tiefe 0,100mm $\frac{1}{400}$ & $\frac{1}{25}$ qmm, UK) in a light microscope (Olympus CH-2 Binocular Microscope, Japan). Six 30mL diluted CCMP374 cultures were set up for each of the three virus strains. Different volumes of the viral lysates were added to the flasks, using 5% (1500µL), 2.5% (750µL), 1% (300µL), 0,5% (150µL) and 0,25% (75µL) of the culture volume in order to achieve a good range. As 10% viral lysate was used during the propagation, it was used as a baseline, meaning the different volumes of viral lysates was supplemented with media to achieve the same final volume of 33mL. Control cultures were added 3mL growth media.

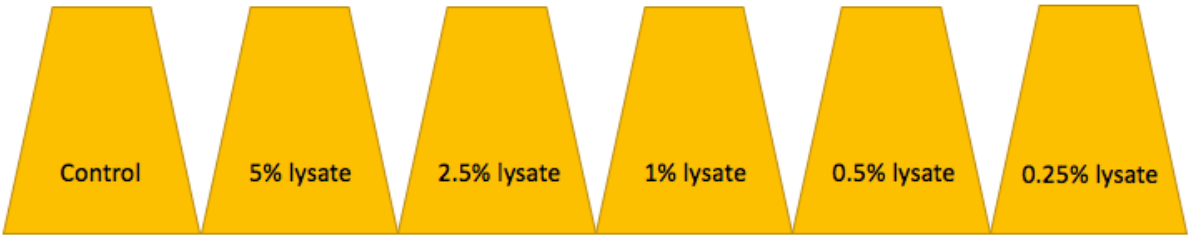

Figure 4. Illustration of the one-step growth curve experiment, where all flasks were added 30mL exponentially growing culture of *E. huxleyi* strain CCMP374. Separately, fresh lysates of the EhV strains 99B1, 208 and 86 were added to the flasks at various volumes based on the percentage of the total culture volume. The cultures were supplemented with media to achieve the same volume of 33mL. The control flasks were added 3mL media.

2.2.2 Cross-infection patterns

The three host strains CCMP374, CCMP371 and B were cross-infected with the three virus strains EhV -99B1, -208 and -86 in triplicates, infected with the lowest MOI needed to maintain a one-step growth curve (see previous section 2.2.1). Viral lysates were supplemented with media in order to achieve the same final volume of 33mL. Triplicates of control cultures for each host was added 3mL media. All cultures had a starting density of ~5 x 10^5 cells/mL to replicate the starting density of the one-step growth experiment. Culture flasks were gently stirred twice before any subsampling.

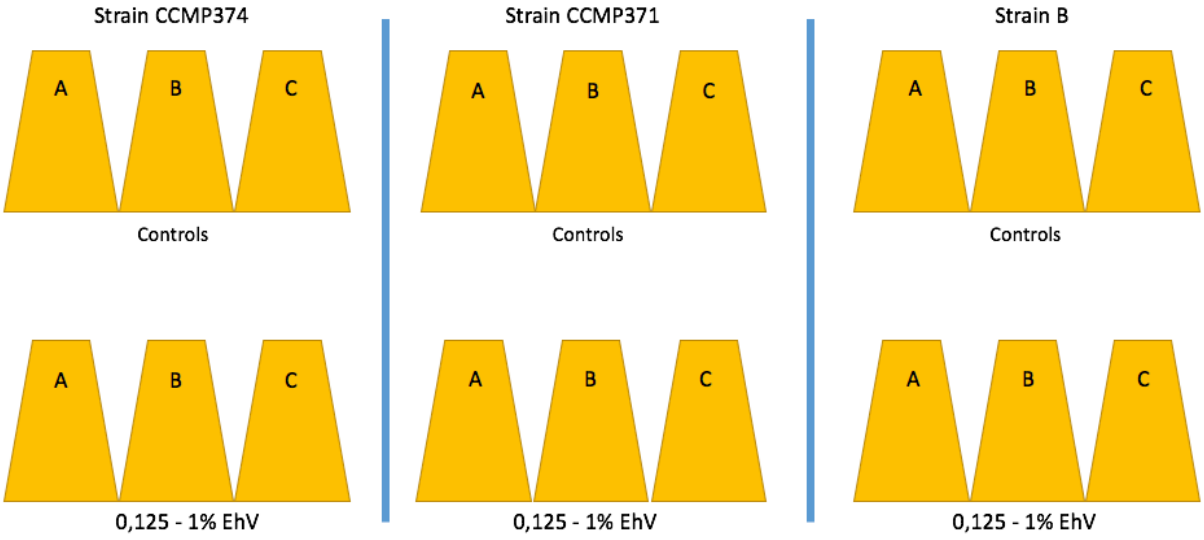

Figure 5. The minimum MOI needed to maintain a one-step growth curve for each of the virus strains (EhV 99B1, 208 and 86) were added separately to 30mL cultures containing the host strains CCMP374, CCMP371 and B, and were supplemented with media to achieve the final volume of 33mL, all in triplicates. Triplicates of 30mL control cultures were added 3mL media.

2.3 Counts and measurements

2.3.1 Viral and algae flow cytometric counts (FCM)

Algae and virus abundance were determined using FACSCalibur BC flow cytometer (Becton-Dickinson, Bioscience, Franklin Lakes, NJ, USA) where 1mL was subsampled every day including the first day (D0-D3) for both virus and algae count. Virus concentrations were also determined for the initial viral lysate used in the setup of each experiment. Virus samples were fixed with 20µL glutaraldehyde (25%) for at least 30 min at 4°C, followed by being snap-frozen and stored in liquid nitrogen (~-200°C). Prior to counting, the samples were thawed, serially diluted 10, 100, 500, 1000, 5000 x dilutions in 0.2µm filtered TE-buffer (10:1 mM Tris:EDTA, pH 8), and stained with 10µL SYBR Green I 100x diluted (Life technologies™, S7567, Canada) for 10 minutes in water bath at 80°C before being cooled in room temperature for at least 10 minutes. The stained samples were analyzed in the Flow Cytometer (FCM) set at medium flow rate for 60s using CellQuest Pro Software (BD Bioscience) as described in Marie et al., 1999. Virus populations were recognized and counted based on side scatter (SSC) and fluorescent properties. Using non-fixed samples, algal populations were recognized and counted based on chlorophyll pigments and side scatter properties, where the FCM were set at high flow rate for 300s, as described in Larsen et al., 2001. Multiplicity of infection (MOI) was determined by dividing the average initial virus concentration on the average initial cell concentration. Burst-sizes could be estimated by dividing the final virus concentration with the initial cell concentration as one-step growth experiments were conducted.

2.3.2 Most Probable Number (MPN)

The most probable number (MPN) method was used in order to determine the quantity of infectious virus particles towards *E. huxleyi* strains CCMP374, CCMP371 and B. At day 0-3, 200µL of infected cultures were subsampled. The initial virus lysates (used to infect the cultures) were also subsampled, but only at day 0. All subsamples were serially diluted 5-folds in sterile seawater. Exponentially growing cultures of each host was diluted to ~5 x 10^5 cells/mL and 140µL was loaded in each well of a VWR 96-well tissue culture plate. The columns on the plate consisted of 8 wells, where each well of a column was loaded with 10µL of serially diluted subsample, having the first column as control by adding 10µL seawater and

the second column undiluted subsample. All plates were sealed by parafilm to reduce evaporation and incubated at 16°C 14:10 light:dark cycle with shading allowing ~33 µmol photons m^{-2} s^{-1} to pass. The plates were read after both 5 and 7 days of incubation using a plate reader (PerkinElmer EnSpire™ 2300 Multilabel Reader, Turku, Finland), set to "In vivo fluorescence 460/680nm". Wells were considered lysed when the *in situ* relative fluorescence of a well was below 50% compared to the control column. However, due to variations within the plates, some of them had to be assessed manually. The most probable number was calculated using MPN calculation program, version 5, 2017 in Microsoft® Excel for Mac, version 16.19, 2018 (Jarvis et al., 2010a).

2.4 Mesocosm Experiment

A mesocosm experiment funded by Aquacosm (funding from the European Union's Horizon 2020 research and innovation program under grant agreement No 731065) and the – VIMS – Ehux project ('The Vardi Group' http://www.weizmann.ac.il/plants/vardi/home) was conducted in Raunefjorden, 200 meters ashore from Espegrend Marine Research Field Station located near Bergen, Norway (60.269664°N; 5.218729°E) during 22. May – 15. June 2018. The experiment consisted of six mesocosm bags, where three parallels were covered with a transparent sheath to enable aerosol collection. The bags were 2m wide and 4m deep ($11m^3$) and were made of 0.15mm thick polyethylene with a 90% light penetration. They were filled with seawater from 2m depth, and the water was kept homogenous in the enclosures by means of an airlift (Castberg et al., 2001). All bags were bubbled with air and supplemented daily with nitrate ($NaNO_3$) and phosphorous (K_2HPO_4) to enhance phytoplankton growth. Seawater samples were collected every second day from two non-covered parallel bags (2 and 4) in which an *Emiliania huxleyi* bloom collapsed by viral lysis (Figure 15).

2.4.1 Virus concentration and filtration

Six liter water samples were prefiltered through a 0.45µm pore-size low-protein-binding Durapore membrane filter of 142 mm in diameter (Millipore, Burlington, MA, USA) to remove large particles and some bacteria from the samples. Approximately 15mL of the filtrates were used in determining the infectious particle concentration by MPN method (see 2.4.2 and Figure 6). The remaining filtrates were concentrated (10psig, high speed) to final

volume of ~50mL by QuixStand tangential flow filtration (TFF) system equipped with a 100 000-pore size (NMWC) hollow-fiber cartridge as described by Sandaa et al., 2018 (QuixStand, GE Healthcare Bio-Science AB, Uppsala, Sweden). The filtration system was rinsed and washed according to instructions from manufacturer before and after processing sample water. Aliquots of 1mL virus concentrate were stored at -80°C in cryotubes until further processing.

2.4.2 Most Probable Number (MPN), mesocosm

The 0.45µm prefiltered samples from the two mesocosm bags (bag 2 and 4) were serially diluted 3-folds in sterile seawater (Figure 6; see 2.3.2 for further details regarding MPN setup). Both dilution series were added to three 96-well microtiter plates separately containing 140µL host strains CCMP374, CCMP371 and B with density of ~10^6 cells/mL in each well. Plates were incubated without shading (unlike in 2.3.2) at ~50 µmol photons m^{-2} s^{-1} and were read using plate reader (PerkinElmer EnSpire™ 2300 Multilabel Reader, Turku, Finland) after both 3 and 5 days of incubation. Wells that contained an *in situ* relative fluorescence below 50% compared to control column were considered lysed. The highest diluted sample that resulted in lysis from each row was collected in 0.5mL Eppendorf tubes and stored at -80°C until further processing.

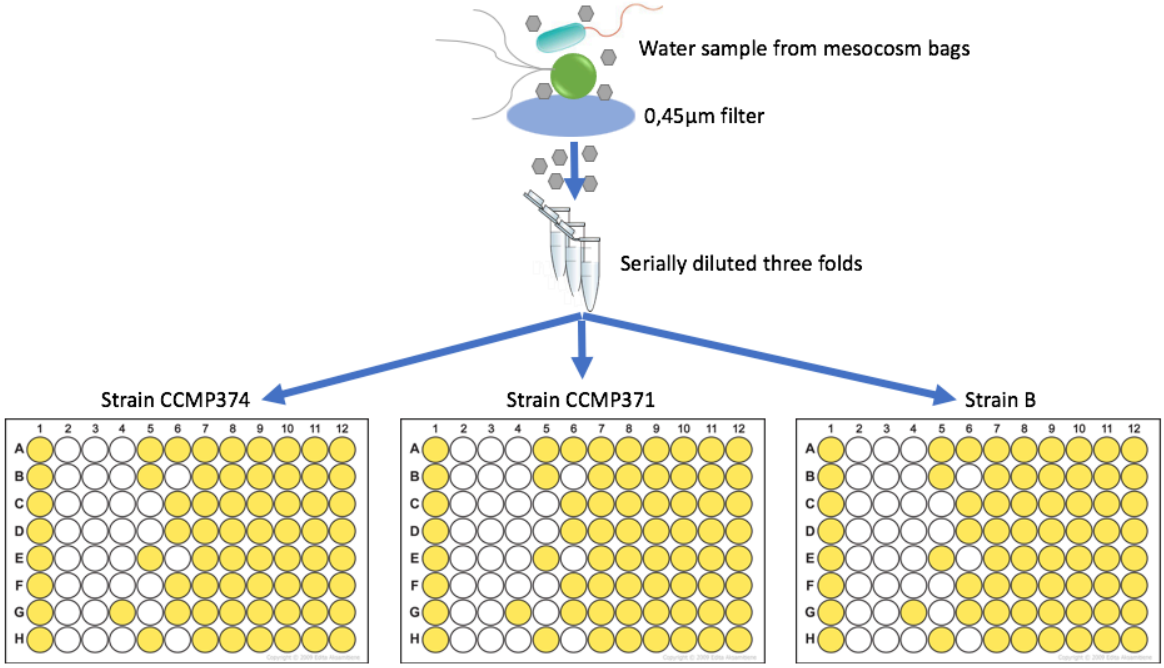

Figure 6. The water samples from the two mesocosm bags were filtered through a 0.45µm filter, removing organisms >0.45µm, while letting smaller particles pass, e.g. viruses. The filtered samples where serially diluted three-folds and added to MPN plates as described in section 2.4.2.

2.4.3 Isolation of Emiliania huxleyi virus

EhVs were isolated from both bags (2 and 4) the last two days of sampling of the mesocosm experiment. They were collected directly from one of the highest diluted wells that resulted in lysis from the MPN (section 2.4.2). The extracted samples were serially diluted 5-folds and plated according to section 2.4.2 on host strain CCMP374. The same procedure was performed again with samples from this new MPN plate, except a 10-fold dilution was used instead. Extraction of the highest diluted well that resulted in lysis was gradually added to larger culture volumes to increase the amount of EhV isolate. The EhV isolates were stored at 4°C.

2.4.4 DNA isolation

DNA isolation protocol was performed on concentrated virus samples (section 2.4.1) collected directly from the two mesocosm bags (2 and 4) as described in Sandaa et al., 2018. Additionally, DNA isolation was performed on the highest diluted column on the MPN plates that resulted in lysis, as well as on the isolated virus strains (sections 2.4.2 and 2.4.3, respectively). Samples were pooled together when two or more wells had lysed in the same column. Using reverse pipetting technique, the volume for these samples were estimated, and if below 500µL, nuclease free water was added to reach this volume.

The frozen virus samples (either 500µL or 1000µL) were incubated at 90°C on heat block for 3 x 2 minutes, placing the samples on ice in between for 2 minutes. For 500µL samples, 20µL 0.5 M EDTA (pH8; Appendix B.2) was added to increase pH and was mixed by vortex. Additionally, 5µL proteinase K (Sigma-Aldrich, SLBV3838, St. Louis, USA), diluted in nuclease free water (10mg/mL), was added to break down viral capsids and was mixed by vortex before being incubated for 10 min in water bath at 55°C. Finally, 25µL 10% SDS (Sodium Dodecyl Sulfate) was added in order to dissolve membrane lipids and the samples were incubated further 1h at 55°C. The isolated DNA was purified using Zymo DNA Clean and Concentrator™-10 kit (Zymo Research, Irvine, CA, USA), according to protocol from the manufacturer. Presence of DNA was confirmed by using Qubit® 2.0 Fluorometer (Invitrogen, Singapore) following the instructions set by manufacturer. Samples were stored in fridge at 4°C until the following day.

2.4.5 PCR reaction

The isolated DNA was prepared for PCR amplification using primers targeting a part of the EhVs major capsid gene (*mcp*) (Rowe et al., 2011). A Phusion 50µL reaction with 2µL template was prepared using MCP-NN-F1 (5'- nnn nnn GTC TTC GTA CCA GAA GCA CTC GCT-3') and MCP-NN-R1 (5'-nnn nnn ACG CCT CGG TGT ACG CAC CCT CA-3') primer set. 2 µL of each template was loaded into PCR tubes (with parallels) and two separate PCR tube was added 2µL EhV-374 (positive control) and nuclease free water (negative control). Templates, positive- and negative control were mixed with 48µL reaction mixture (Table 1). Each PCR tube was mixed by vortex and spun down for 3-5 seconds (VWR™ Galaxy MiniStar, E_K 26 Joules, Korea) to center the liquid. PCR samples were run in a PCR machine (BIO-RAD, iCycler™ Thermal Cycler, USA) set according to Table 2. PCR 1 products (14 cycles) were stored at -80°C and later shipped on dry ice to Weizmann institute to be sequenced using Illumina MiSeq platforming and v3 PE300 sequencing chemistry. PCR 2 products (30 cycles) were prepared for agarose gel electrophoresis (DGGE).

A 1.5% agarose gel was set up, mixing 0.8g Agarose (SeaKem® LE Agarose, 50004, USA) with 60 mL 1 x TAE Buffer (40mM tris, 20mM acetic acid, 2.5mM EDTA) in a heat tolerant flask. The solution was heated and stirred in a microwave to dissolve the agarose, followed by adding 2µL 10 000X GelRed™ stain (Biotium, 41003, USA). The solution was cooled down to ~50°C in room temperature. The cooled solution was poured into gel-rack with a 12-well comb and was left to solidify for ~30 minutes. The gel was put in a frozen electrophoresis chamber and was filled with ~250mL 1 x TAE Buffer, until the surface of the gel was fully submerged. 3 µL MassRuler™ DNA Ladder Mix (Thermo Fisher Scientific, SM0403, Lithuania) was loaded on both ends of the gel, while 3µL PCR product, as well as positive and negative control was mixed with ~1 µL MassRuler™ LD (Thermo Fisher Scientific, SM0403, Lithuania) on sterile parafilm before being loaded onto the gel. The gel-electrophoresis was set at 200V for ~30 min. The complete gel was loaded into BIO RAD Molecular Imager® (ChemiDoc XRS™) and a fluorescent image was obtained using Image Lab™ software (see example in Appendix C.1, Figure C-1).

Table 1. PCR Reaction Mixture

Forward Primer (10µM)	2.5 µL
Reverse Primer (10µM)	2.5 µL
2 x Phusion Master Mix (NEB, M0530)	25 µL
Template DNA	2 µL
Nuclease free water	18 µL
Total	50 µL

Table 2. Amplification of the *mcp* gene

Reaction Steps	**Temperature °C**	**Time**	**PCR 1 (cycles)**	**PCR 2 (cycles)**
Initial Denaturation	98	30 s	1	1
Denaturation	98	5 s		
Annealing	65	60 s	14	14 + 16
Extension	74	90 s		
Final Extension	74	5 min	1	1
End	4	∞		

2.4.6 Cloning and sequencing

PCR products from the isolated virus strains (sections 2.4.4 and 2.4.5) were prepared for cloning using the StrataClone™ PCR Cloning Kit (240205, California, USA). A ligation reaction was set up where 3µL cloning-buffer, 2µL PCR-product and 1µL vector was added chronologically and mixed by a gentle swirl using the tip of a pipette. After 5 min incubation in room temperature, 1µL was added to a tube with thawed competent cells and was carefully mixed followed by a 20 min transformation reaction on ice. The cells were given a heat-shock by incubating them in water bath at 42°C for 45s followed by incubation on ice for 2 min. The transformation reaction cells were added 250µL LB-medium (Appendix B.3) preheated at 42°C and was incubated for over 1 hour at 37°C. Premade LA plates with 100 µg/mL Ampicillin (Appendix B.3) plated with 40µL 2% X-gal (0.2g 5-bromo-4-chloro-3-inodlyl-®-D-galactopyranoside in 10mL dimethylformamide (DMF), stored at -20°C), were plated with both 20 and 40µL of each transform reaction cells onto separate plates and incubated overnight at 37°C.

To check for positive clones, three white colonies were picked from each plate using sterile toothpick. Separately, they were mixed with 25µL HotStarTaq® reaction mix (Table 3) in PCR tubes, before being placed in the PCR machine in order to amplify the inserted *mcp* gene

using the PCR program shown in Table 4. The PCR products were run on a 1.5% agarose gel electrophoresis as described in section 2.4.5.

PCR products with a strong visual band on the agarose gel (Appendix C.1, Figure C-2), were purified by mixing 5µL PCR product with 2µL 1-step ExoStar (illustra™ ExoProStar™, US77705V, GE Healthcare) in order to remove unincorporated primers and nucleotides. The enzymes in the ExoStar reaction was activated with an initial step of 37°C for 15min, followed by deactivation at 80°C for 15min and ending at 4°C using the PCR-machine. Presence of adequate quantity of DNA in the purified samples were confirmed by measuring the DNA concentration using the Qubit® 2.0 Fluorometer as described in section 2.4.4.

A library prep was set up using Big-Dye Cycling sequencing kit (Big-Dye version 3.1 and sequencing buffer were provided by the Sequencing Facility, MBI, UiB). Separately, 2µL purified PCR-product was added to PCR-tubes, each containing 8µL Big-Dye master mix (Table 5). The PCR-tubes were spun down (3-5s) and placed in the PCR machine following the program in Table 6. After PCR reaction, 10µL of nuclease free water was added to each PCR-product before being placed in a -20°C freezer. The libraries were sequenced at Sequencing Facility, MBI, University of Bergen (Thormølensgate 55, 5008 Bergen, Norway) using the Sanger sequencing method.

Table 3. Master Mix HotStarTaq

M13 Forward primer (10µM)	1.25 µL
M13 Reverse primer (10µM)	1.25 µL
HotStarTaq Master Mix	12.5 µL
Nuclease free water	10 µL
Total	25 µL

Table 4. M13 PCR Settings

Reaction Steps	**Temperature °C**	**Time**	**PCR 1 (cycles)**
Initial Denaturation	94	10 min	1
Denaturation	94	1 min	
Annealing	55	1 min	30
Extension	72	1 min	
Final Extension	72	10 min	1
End	4	∞	

Table 5. Master Mix preparation for sequencing – Big-Dye

Big-Dye (version 3.1)	1 µL
Sequencing Buffer	1 µL
M13 Forward Primer (1µM)	3.2 µL
Nuclease free water	2.8 µL
Total	8 µL

Table 6. PCR setting for preparation for sequencing

Reaction Steps	Temperature °C	Time	Cycles
Initial Denaturation	96	5 min	1
Denaturation	96	10 s	
Annealing	55	5 s	25
Extension	60	4 min	
End	4	∞	

2.5 Statistics, calculations and software

All graph representations were created using R Software (R Core Team, 2017. R: A language and environment for statistical computing. R Foundation for Statistical Computing, Vienna, Austria. URL <https://www.R-project.org/>), except for graphs with dual y-axis, which were made using Prism 8 for macOS, GraphPad software©, Inc. Calculations were executed in Microsoft® Excel for macOS, Version v16. The statistical analyses were completed using StatPlus:mac, AnalystSoft Inc. - statistical analysis program for macOS®. Version v6. See <http://www.analystsoft.com/en/>.

OTU tables were produced from the Illumina sequences that were quality trimmed using Dada2 pipeline by Flora Vincent (Vardi Group – Weissman Institute). DNA sequences were first aligned for SNP (Single Nucleotide Polymorphism) analysis using clustalW (Thompson et al., 1994), through GenomeNet, Kyoto University Bioinformatics Center, URL < https://www.genome.jp>. A phylogenetic tree was constructed using Maximum Likelihood method based on the Tamura-Nei model with 500 bootstrap replications in MEGA7 for macOS X (Kumar et al., 2016) aligned by clustalW.

3 Results

3.1 Defining the *minimum MOI that maintains a one-step growth curve*

Algal count from host strain CCMP374 separately infected with the three virus strains EhV -99B1, -208 and -86 revealed that different relative MOI-concentrations were necessary to maintain a one-step growth curve with minimal excess virus particles. The added MOI-concentrations are relative, as they might vary if culture conditions are not replicated or due to biological variations. The minimum relative MOI-concentration was determined by visual observation of the decline in algal cell counts between days 2 and 3 (Figure 7), targeting the MOI that caused a divergence in the slope from those treatments with too high or too low MOIs. All virus counts are averaged over their technical replicates and excluded standard deviation for simplicity.

The initial cell-concentration of host CCMP374 in Figure 7 ranged from 3.0 to 3.4 x 10^5 cells/mL (average 3.2 x 10^5 cells/mL) in all culture flasks. The final cell-concentrations in the control cultures ranged between 1.4-1.9 x 10^6 cells/mL. The initial viral lysates used in the experiments to infect the cultures were estimated to 4.25, 3.39 and 3.55 x 10^8 VLPs/mL for EhV strains 99B1, 208 and 86, respectively.

EhV-99B1 infected cultures added relative MOI-concentrations of 5%, 2.5%, 1%, 0.5% and 0.25%, had final cell-concentrations of 3.5 x 10^3, 4.8 x 10^3, 6.9 x 10^3, 1.0 x 10^4 and 1.8 x 10^4 cells/mL, respectively (Figure 7, upper left graph). The initial and final virus concentrations in these culture flasks were 1.8 x 10^7, 9.1 x 10^6, 4.0 x 10^6, 2.4 x 10^6 and 1.3 x 10^6 VLPs/mL, and 1.7, 1.8, 2.3, 1.8 and 2.3 x 10^8 VLPs/mL, respectively (Figure 7, lower left graph). As the number of EhV-99B1 was too high to determine the lowest number VLPs necessary to maintain a one-step growth curve, a new experiment was performed with a higher dilution of the viral lysate (Figure 8). The new final cell concentrations in culture flasks added relative MOI-concentrations of 0.5%, 0.25% and 0.125% were 8.7 x 10^3, 9.1 x 10^3 and 1.9 x 10^4 cells/mL, respectively (with average initial cell concentrations of 2.7 x 10^5 cells/mL). The initial and final virus concentrations in these culture flasks were 1.4 x 10^6, 7.9 x 10^5 and 3.4 x 10^5 VLPs/mL, and 3.9, 2.5 and 2.4 x 10^8, VLPs/mL, respectively. Using the final cell numbers of cultures added various relative MOI-concentrations of EhV-99B1 together with the visual slopes in Figure 8 (left graph), there is a considerable increase when using 0.125%

relative MOI-concentration (1.9 x 10^4 cells/mL) in comparison to higher relative MOI-concentrations (0.5% and 0.25% with 8.7 x 10^3, 9.1 x 10^3 cells/mL, respectively). This indicates 0.125% is the threshold for the relative MOI-concentrations necessary to maintain a one-step growth curve. The MOI value was calculated for this relative MOI-concentration and estimated to be 1.26 virus particles per host cell.

When infecting the same host strain with EhV-208 with the same relative MOI-concentrations (5%, 2.5%, 1%, 0.5% and 0.25%), we measured a final cell concentrations of 4.8 x 10^3, 7.3 x 10^3, 8.3 x 10^3, 1.6 x 10^4 and 3.1 x 10^4 cells/mL, respectively (Figure 7, middle upper graph). The initial and final virus concentrations in the same culture flasks were 1.5 x 10^7, 5.9 x 10^6, 2.9 x 10^6, 1.7 x 10^6 and 1.1 x 10^6 VLPs/mL, and 1.1, 1.1, 1.4, 1.4 and 1.9 x 10^8 VLPs/mL, respectively. A higher relative MOI-concentration was necessary for EhV-208 to produce a one-step growth curve. The considerable increase in final cell concentration and the visual deviation of the slope in Figure 7 (upper-middle graph) at 0.5% relative MOI concentration (1.6 x 10^4 cells/mL) compared to higher relative MOI concentrations (5%, 2.5% and 1% with 4.8 x 10^3, 7.3 x 10^3 and 8.3 x 10^3 cells/mL, respectively) indicates that 0.5% is the threshold for the relative MOI-concentrations necessary to maintain a one-step growth curve. The MOI value was calculated for this relative MOI-concentration and estimated to be 5.31 virus particles per host cell.

The third virus strain, EhV-86, that was used in the infection of the same host strain added with relative MOI-concentrations of 5%, 2.5%, 1%, 0.5% and 0.25%, had final cell concentrations of 4.7 x 10^3, 4.5 x 10^3, 1.3 x 10^4, 3.6 x 10^4 and 4.3 x 10^4 cells/mL, respectively (Figure 7, upper-right graph). The initial and final virus concentrations in these culture flasks were 1.5 x 10^7, 7.1 x 10^6, 3.4 x 10^6, 1.9 x 10^6 and 1.1 x 10^6 VLPs/mL, and 1.2, 1.0, 1.4, 1.7 and 1.7 x 10^8 VLPs/mL, respectively. For EhV-86, both the visual deviation of the slope in Figure 7 (upper-right graph) and the significant increase in final cell number at 1% relative MOI-concentration (1.3 x 10^4 cells/mL) compared to the higher relative MOI-concentrations (5% and 2.5% with 4.7 and 4.5 x 10^3 cells/mL, respectively), suggests that 1% is the minimum relative MOI-concentration needed to produce a one-step growth curve. The MOI value for 1% relative MOI-concentration was 10.63 virus particles per host cell.

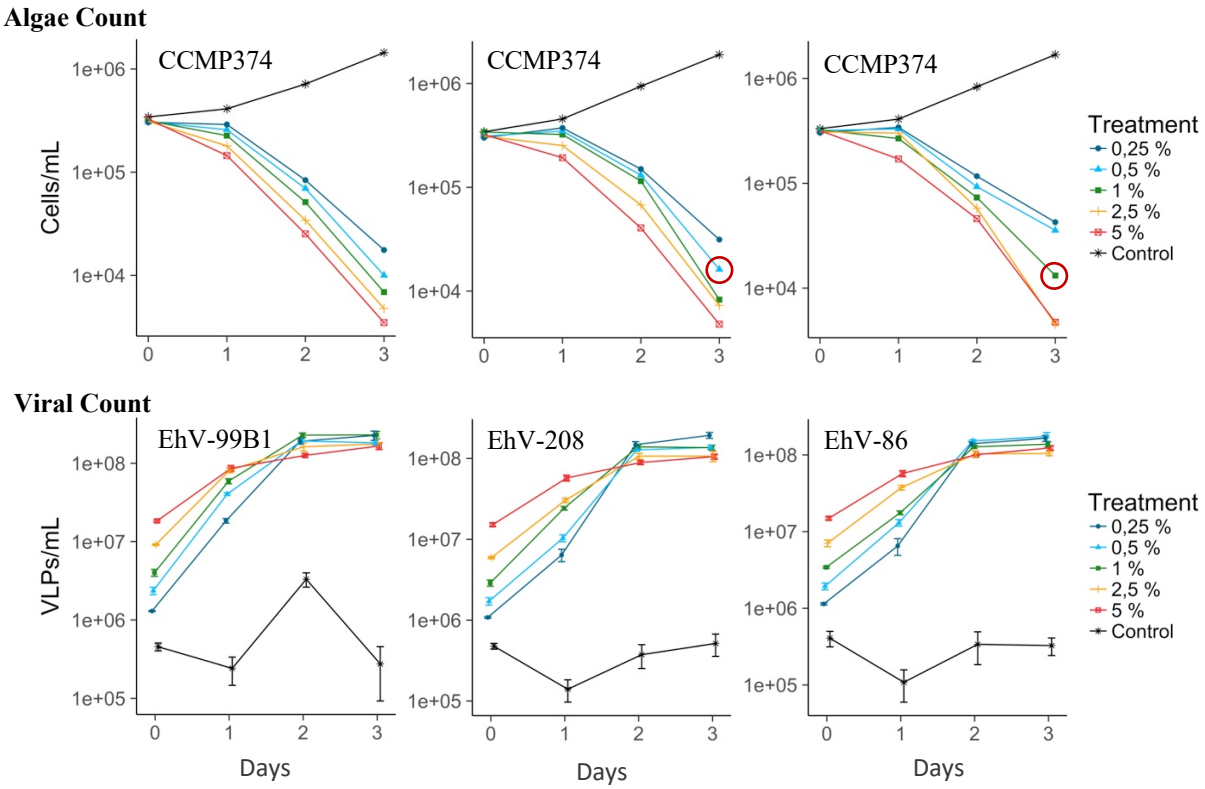

Figure 7. The three upper graphs represent algae count of CCMP374 cultures infected with various relative MOI-concentrations (percent of culture volume) of EhV -99B1, -208 and -86, respectively, measured over three days. The corresponding graphs below represent the viral count from these infected cultures as well as background noise in non-infected control cultures. The minimum relative MOI-concentration needed to produce a one-step growth curve has been suggested with a red circle at day 3. Note that the lower limit for EhV-99B1 on CCMP374 seemed to be less than the relative MOI-concentrations tested and is not indicated here (see Figure 8). Error bars on viral counts represent standard deviation.

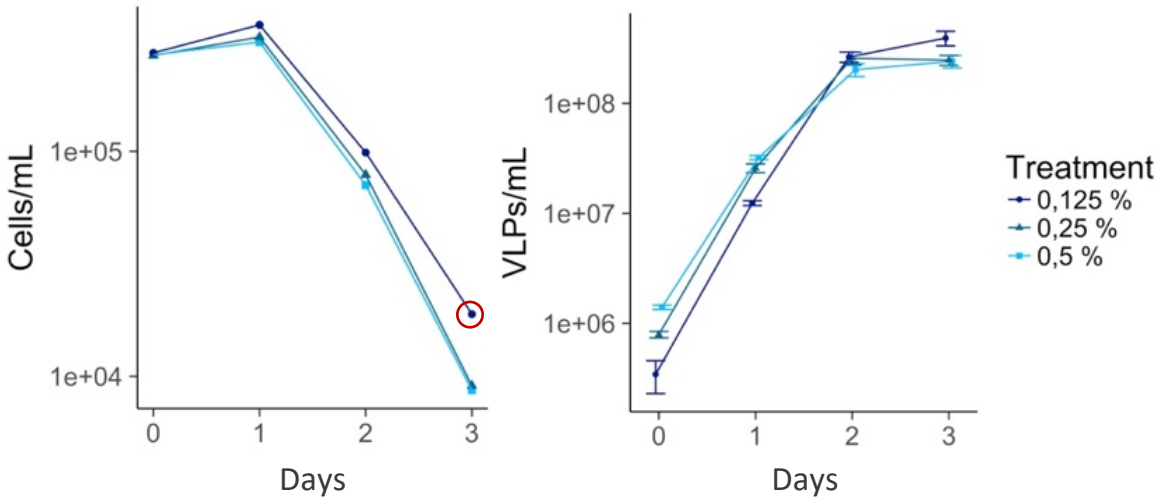

Figure 8. CCMP374 infected with EhV-99B1, with various relative MOI-concentrations (percent of culture volume). The left graph represents algae count and the right graph represents virus count of the infected cultures. The minimum relative MOI-concentration needed to produce a one-step growth curve has been suggested with a red circle at day 3. Error bars on viral counts represent standard deviation.

3.2 Cross infection patterns

3.2.1 Initial experiments

Prior to the cross-infection of the experiments in section 3.2.2, each of the initial viral lysates (EhV -99B1, -208 and -86) used to infect the cultures in the cross-infection, were estimated for concentration of both VLP and infectious particle towards the three host strains (CCMP374, CCMP371 and B). Initial EhV-99B1 lysate had 2.65 x 10^8 VLPs/mL, and 4.7, 6.1 and 9.8 x 10^5 MPN/mL towards host strains CCMP374, CCMP371 and B, respectively. Initial EhV-208 lysate had 1.90 x 10^8 VLPs/mL and 2.4 x 10^6 MPN/mL towards CCMP374 only. Initial EhV-86 lysate had 3.28 x 10^8 VLPs/mL and 5.4 x 10^5 MPN/mL towards CCMP374 only.

3.2.2 Cross-infection

Both the cell and viral counts presented in the following sections are averaged from the triplicates and for simplicity do not include standard error (coefficient of variation (CV) for the standard error (SE) was SE (CV_{Algae}) = 5.3% and SE (CV_{Virus}) = 6.7%).

EhV-99B1

The starting cell-concentrations of host CCMP374, CCMP371 and B infected with EhV-99B1 were 4.0, 3.6 and 3.4 x 10^5 cells/mL, and increased to 2.1, 1.8 and 1.6 x 10^6 cells/mL, respectively at day 3 in the controls (Figure 9, upper graphs). In the CCMP374 cultures infected with EhV-99B1 the number decreased to 3.6 x 10^4 cells/mL at day 3. CCMP371 and B infected cultures both increased at day 2 to 4.5 and 4.1 x 10^5, before decreasing at day 3 to 6.9 and 8.4 x 10^4 cells/mL, respectively.

The number of virus particles (VLP) in the CCMP374, CCMP371 and B infected experiment were 4.4, 3.3 and 3.5 x 10^5 VLPs/mL, respectively at day 0 and increased to 3.2, 1.5 and 1.7 x 10^8 VLPs/mL, respectively at day 3 (Figure 9, lower graphs).

The infectious particles (MPN) in CCMP374, CCMP371 and B cultures were 9.0 x 10^2, 7.3 x 10^2 and 1.8 x 10^3 MPN/mL, respectively at day 0 and increased to 1.0, 1.0 and 2.0 x 10^6 MPN/mL, respectively at day 3.

The final yield of both virus and infectious particles (VLP and MPN; day 3) of EhV-99B1 propagated on host cultures CCMP374, CCMP371 and B are compared visually in Figure 10 (significance values shown in Table 7). Day 3 MPN concentrations of EhV-99B1 propagated on host strains CCMP374 and CCMP371 are not statistically different (p=0,96), however, the final number of VLPs between these two strains are significant (p=0). Both the final MPN and VLP concentrations are significantly different when propagated on host CCMP374 and B (p=0,00017 and p=0, respectively). The same is true for both MPN and VLP concentrations when propagating on host CCMP371 compared to B (p=0,00017 and p=0,0018). Note that there are no significant differences in VLP concentrations at day 0 when the cultures were infected, suggesting that all cultures had the same initial viral abundance.

Table 8 represents the burst sizes and the final (day 3) percentages of infectious particles (MPN) to the total number of virus particles (VLP) for the three host strains infected with EhV-99B1. The percentage of infectious particles found in infected cultures of host strains CCMP374, CCMP371 and B were 0.32%, 0.68% and 1.20%, respectively. The virus burst sizes on these host strains were 816, 419 and 491 virus particles per host cells, respectively (see Table 8 for SE values).

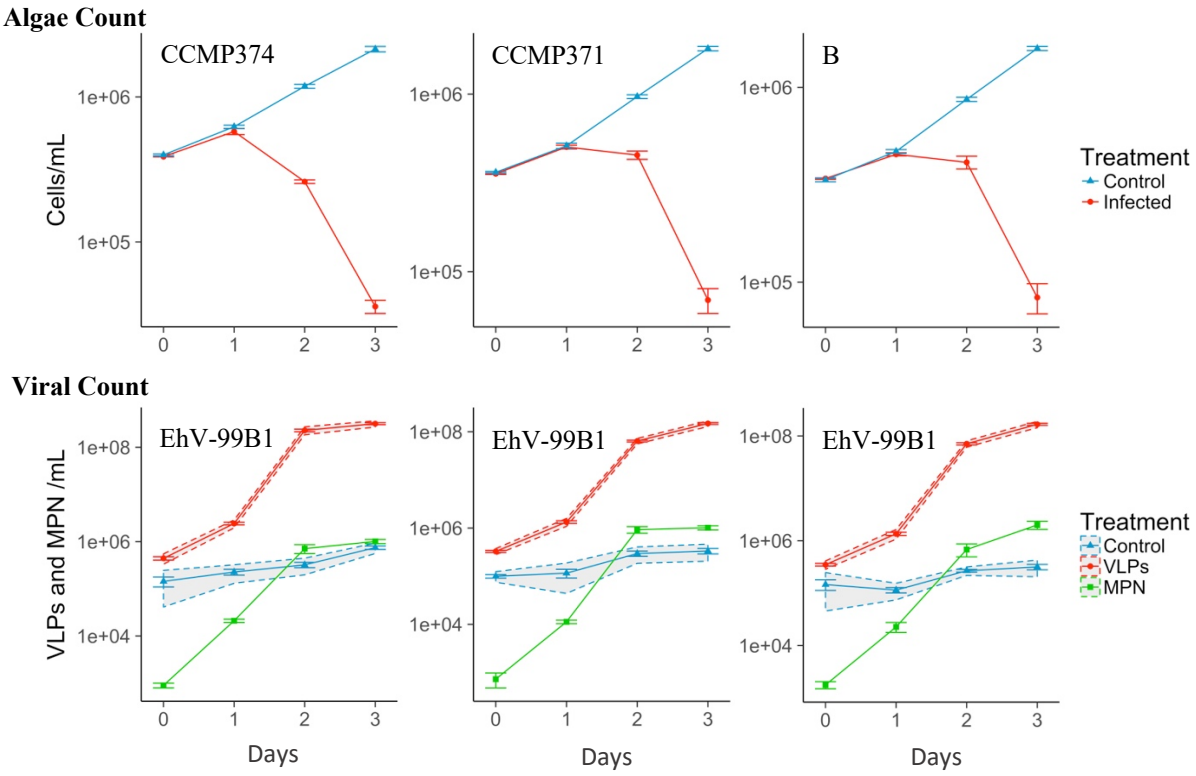

Figure 9. The three upper graphs represent algae count of host strains CCMP374, CCMP371 and B infected with EhV-99B1 and control cultures all in triplicates (averaged with standard error). The corresponding graphs below represent average values of both VLPs and MPN per mL, along with background noise in control cultures. Standard error is represented as an error bar for both MPN and VLPs, while standard deviation is represented as a ribbon for VLPs only.

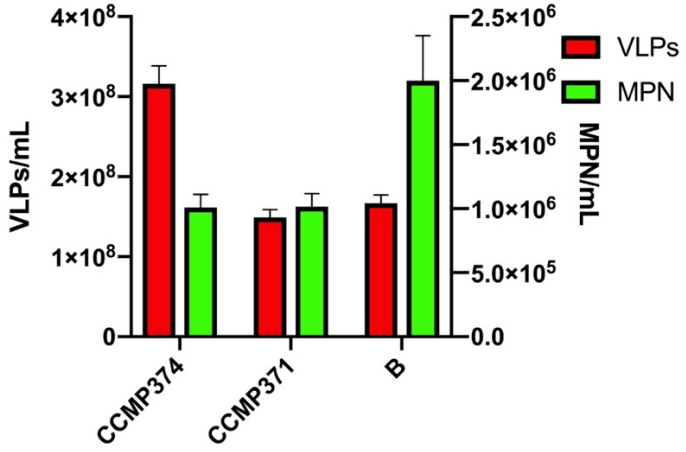

Figure 10. Host cultures CCMP374, CCMP371 and B infected by EhV-99B1 showing virus like particles (VLPs in red) and infectious particles (MPN in green) produced three days post-infection with dual y-axis (VLPs left axis, MPN right axis). Error bars represent standard error.

Table 7. Host cultures CCMP374, CCMP371 and B infected with EhV-99B1 statistically compared using two-way ANOVA analysis tool receiving p-values for both MPN and VLPs between the strains at the different time-points. Significance is represented with red color.

Day	Comparing	p-value of MPN	p-value of EhV
0	CCMP374	0,99894	0,99198
1	VS	0,93944	0,92426
2	CCMP371	0,10119	**0**
3		0,95849	**0**
0	CCMP374	0,99686	0,99354
1	VS	0,99399	0,92690
2	B	0,89224	**0**
3		**0,00017**	**0**
0	CCMP371	0,99623	0,99701
1	VS	0,95872	0,99699
2	B	0,26952	0,23591
3		**0,00017**	**0,00183**

Table 8. The percentage of infectious viral particles (MPN) of the total number of viruses produced (VLP) for the three hosts infected with EhV-99B1. Burst-size represents number of VLPs released from each cell with standard error and is based on flow cytometric counts.

Host	MPN/mL	VLPs/mL	Percentage of infectious particles[1]	Burst-Size
CCMP374	$1{,}01 \times 10^6$	$3{,}16 \times 10^8$	0,32%	816 ± 55
CCMP371	$1{,}02 \times 10^6$	$1{,}49 \times 10^8$	0,68%	419 ± 30
B	$2{,}00 \times 10^6$	$1{,}67 \times 10^8$	1,20%	491 ± 33

[1] Calculated by dividing MPN/mL on VLPs/mL and multiplying with 100%

EhV-208

The starting cell-concentrations of host CCMP374, CCMP371 and B infected with EhV-208 were 3.0, 3.6 and 3.6 x 10^5 cells/mL, and increased to 1.7, 2.0 and 2.0 x 10^6 cells/mL, respectively at day 3 in the controls (Figure 11, upper graphs). In the CCMP374 cultures infected with EhV-208 the concentration decreased to 1.1 x 10^4 cells/mL at day 3. CCMP371 and B infected cultures both increased to 1.7 x 10^6 cells/mL at day 3.

The number of virus particles in the CCMP374, CCMP371 and B infected experiment were 8.8, 8.2 and 7.7 x 10^5 VLPs/mL, respectively at day 0 (Figure 11, lower graphs). In

CCMP374 infected cultures the number of virus particles increased to 1.5 x 10^8 VLPs/mL at day 3. CCMP371 and B infected cultures decreased in number of virus particles to 4.4 and 5.4 x 10^5 VLPs/mL, respectively at day 3.

The infectious particles (MPN) in EhV-208 infected CCMP374 cultures were 1.5 x 10^4 MPN/mL at day 0 and increased to 9.1 x 10^5 MPN/mL at day 3 (Figure 11, lower graphs). CCMP371 and B were not susceptible towards EhV-208 and MPN could not be estimated.

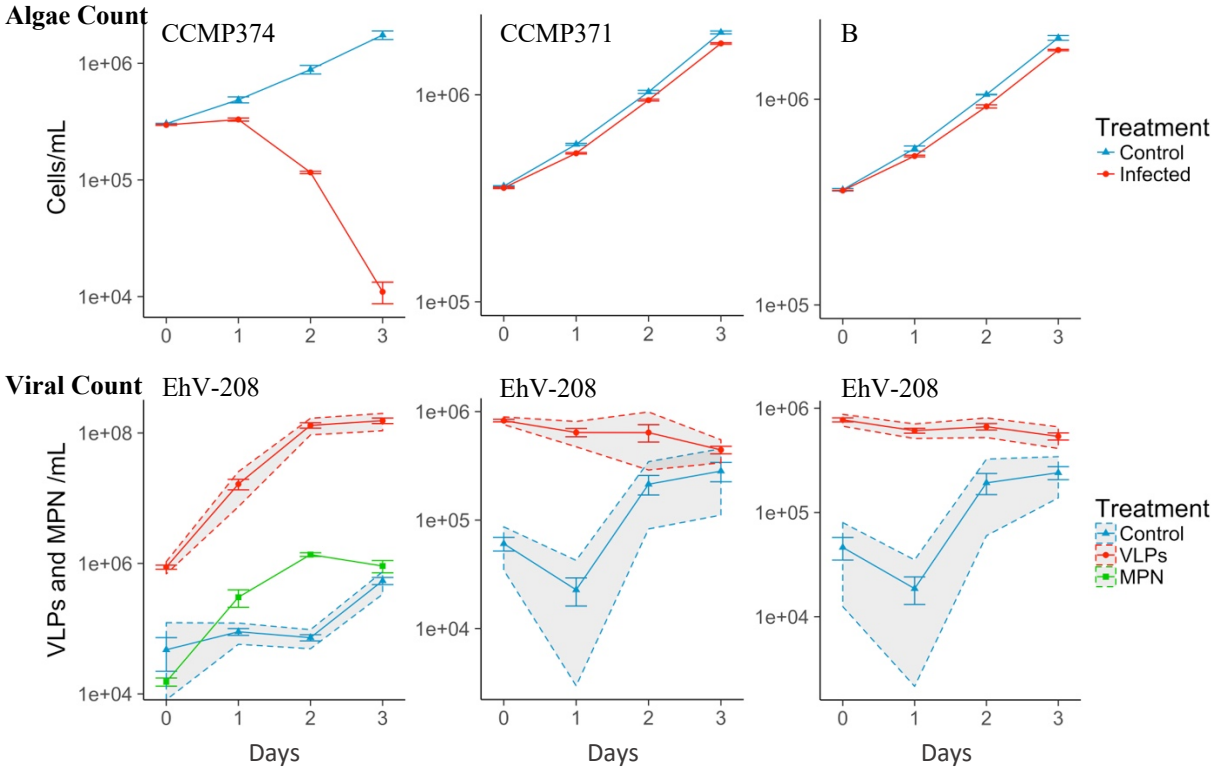

Figure 11. The three upper graphs represent algae count of host strains CCMP374, CCMP371 and B infected with EhV-208 and control cultures all in triplicates (averaged with standard error). The corresponding graphs below represent average values of both VLPs and MPN per mL, along with background noise in control cultures. Standard error is represented as an error bar for both MPN and VLPs, while standard deviation is represented as a ribbon for VLPs only.

EhV-86

The starting cell-concentrations of host CCMP374, CCMP371 and B infected with EhV-86 were 4.0, 4.8 and 3.7 x 10^5 cells/mL, and increased to 1.9, 1.8 and 1.5 x 10^6 cells/mL, respectively at day 3 in the controls (Figure 12, upper graphs). In the CCMP374 infected

cultures the number decreased to 2.2 x 10^4 cells/mL at day 3. CCMP371 and B infected cultures both increased to 1.5 and 1.1 x 10^6 cells/mL, respectively at day 3.

The number of virus particles in the CCMP374, CCMP371 and B infected experiment were 3.1, 2.8 and 2.9 x 10^6 VLPs/mL, respectively at day 0 (Figure 12, lower graphs). In CCMP374 infected cultures the number of virus particles increased to 8.3 x 10^7 VLPs/mL at day 3. CCMP371 and B infected cultures decreased in number of virus particles to 1.4 and 1.3 x 10^6 VLPs/mL, respectively at day 3.

The infectious particles (MPN) in CCMP374 infected cultures were 8.1 x 10^3 MPN/mL at day 0 (Figure 12, lower graphs). The infectious particles in this culture increased to 4.0 x 10^5 MPN/mL at day 2, but thereafter decreased to 2.8 x 10^5 MPN/mL at day 3. CCMP371 and B were not susceptible towards EhV-86 and MPN values could not be estimated.

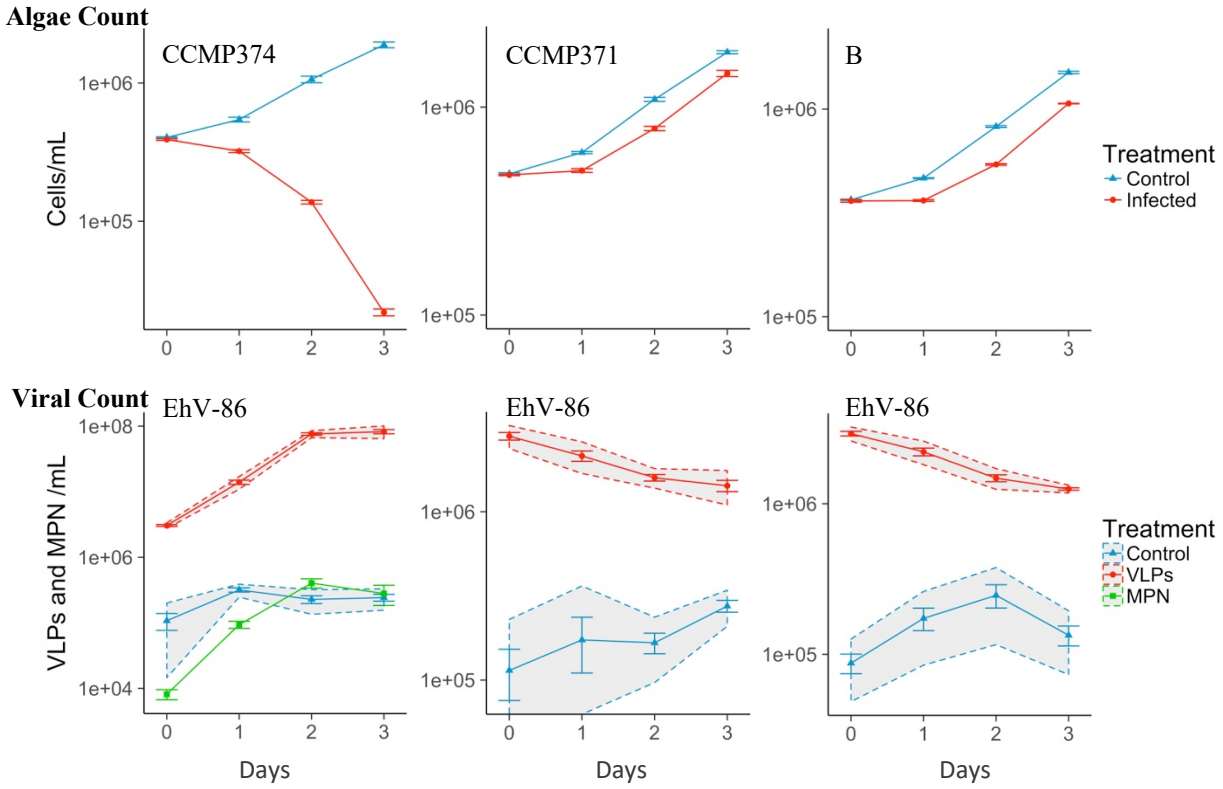

Figure 12. The three upper graphs represent algae count of host strains CCMP374, CCMP371 and B infected with EhV-86 and control cultures all in triplicates (averaged with standard error). The corresponding graphs below represent average values of both VLPs and MPN per mL, along with background noise in control cultures. Standard error is represented as an error bar for both MPN and VLPs, while standard deviation is represented as a ribbon for VLPs only.

In situ relative fluorescence

Virus propagation did not occur in MPN plates containing CCMP371 or B infected separately with serially diluted EhV-208 and 86 lysates. Figure 13 shows the average *in situ* relative fluorescence for each column of the MPN plates added with serially diluted initial virus lysate (EhV -208 and -86) used to infect the cultures in the cross-infection (3.2.1). Considering the left graph, the first column of the MPN plate added undiluted (5^0) EhV-208 lysate, had a lower average relative fluorescence compared to the next dilution (5^{-1}) for both CCMP371 and B. However, the average relative fluorescence had an overall decrease between dilutions 5^{-4} and 5^{-10} on host CCMP371 followed by an increase in the last dilution 5^{-11}.

The right graph in Figure 13 show the same two host strains (CCMP371 and B) on MPN plates, but added with serially diluted initial EhV-86 lysate instead. The average relative fluorescence for both host strains were lowest in the column added undiluted lysate, but increased steeply in the following two dilutions (5^{-1} and 5^{-2}). Both host strains varied in average relative fluorescence the remaining dilutions, but was most prominent on host B. Figure C-4 in Appendix C.3 show examples of how the graphs are expected to look like if the host are added a virus that can propagate and produce infectious particles (data from the mesocosm).

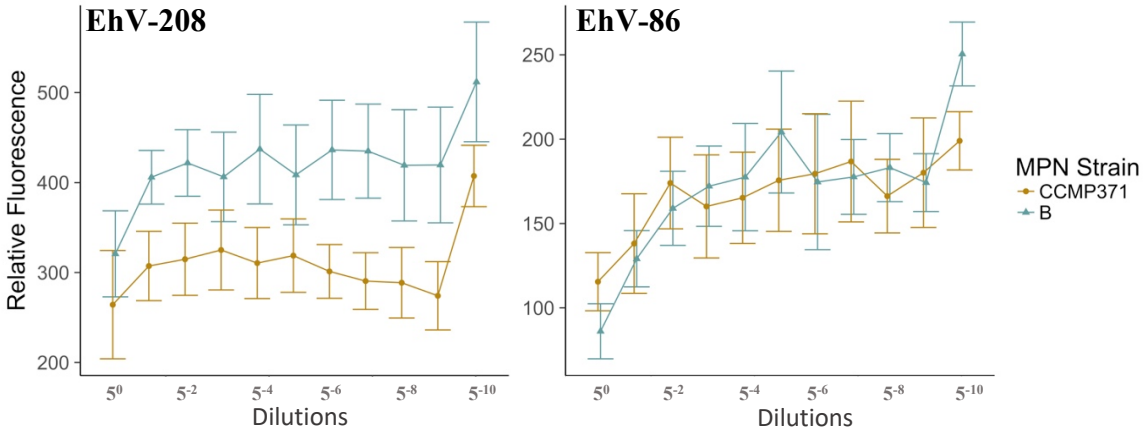

Figure 13. The graph on the left shows the *in situ* relative fluorescence for strains CCMP371 (circular points, dark-yellow line) and B (triangular points, blue line) infected with EhV208, while the right graph shows the same strains infected with EhV-86. Each point on the x-axis represent the average relative fluorescence of all eight wells in a column of the MPN plates with standard error bar. The data points have been dodged (x-axis) to separate them where there is overlap.

CCMP374 and the three virus strains

Host strain CCMP374 was the only host strain to propagate all three virus strains EhV -99B1, -208 and -86. The final (day 3) concentration of virus (VLP) and infectious (MPN) particles propagated on host CCMP374 are visually compared in Figure 14. Significance values from Table 9 represents that the MPN concentrations from infected host strain CCMP374 are not statistically different between EhV -99B1 and -208 at day 3 ($p=0.52$), however, the VLPs concentrations between the two virus strains are significant ($p=4.34 \times 10^{-17}$). Both final MPN and VLP concentrations are statistically significant between EhV -99B1 and -86 ($p=8{,}54 \times 10^{-7}$ and $p=0$, respectively). This is also true for both MPN and VLP concentrations between EhV -208 and -86 ($p=0{,}00007$ and $p=2{,}98 \times 10^{-9}$, respectively). Significance is found between all three virus strains on day 2 of infection (see Table 9 for significance values).

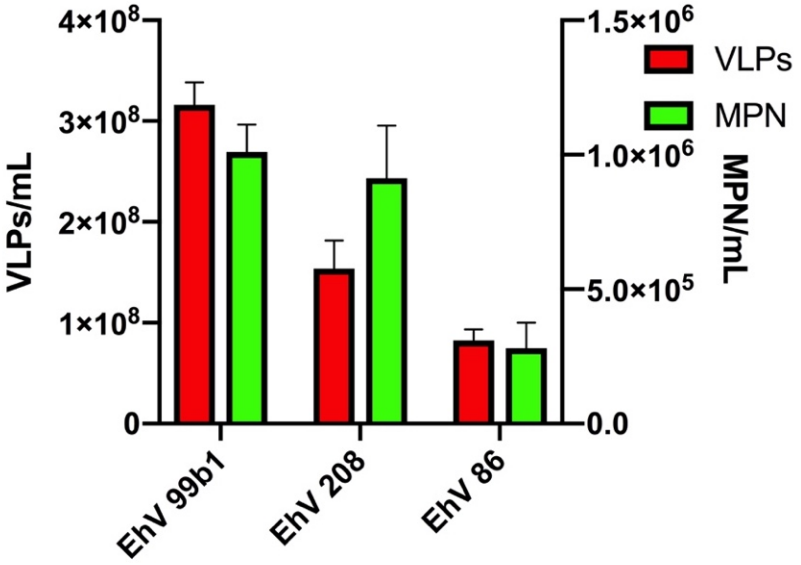

Figure 14. Host culture CCMP374 infected by the three virus strains EhV -99B1, -208 and -86, where the bars represent virus like particles (VLPs in red) and infectious particles (MPN in green) produced three days post-infection with dual y-axis (VLPs left axis, MPN right axis). Error bars represent standard error.

Table 10 represents the burst sizes and the percentage of infectious particles (MPN) to the total number of viruses produced (VLP) for the three virus strains EhV -99B1, -208 and -86 propagated on host CCMP374 at day 3. The percentage of infectious particles found in infected cultures of EhV -99B1, -208 and -86 were 0.32%, 0.59% and 0.34%, respectively. The burst sizes for EhV -99B1, -208 and -86 were 816, 519 and 212 virus particles per host cells, respectively (see Table 10 for SE values).

Table 9. CCMP374 infected cultures added with EhV -99B1, -208 and -86, comparing the strains by means of Two-Way ANOVA to see significant difference in number of infectious particles or VLPs between the strains at the different time-points. Significance is represented in red color.

Day	Comparing	p-value of MPN	p-value of EhV
0	EhV-99B1	0,92298	0,97629
1	VS	0,06892	0,34097
2	EhV-208	**0,00020**	**$5{,}37535 \times 10^{-9}$**
3		0,51938	**$4{,}34222 \times 10^{-17}$**
0	EhV-99B1	0,94716	0,81738
1	VS	0,50789	0,30930
2	EhV-86	**0,00951**	**0**
3		**$8{,}53670 \times 10^{-7}$**	**0**
0	EhV-208	0,95635	0,83666
1	VS	0,12118	0,81375
2	EhV-86	**$2{,}06772 \times 10^{-7}$**	**$1{,}84934 \times 10^{-6}$**
3		**0,00007**	**$2{,}98263 \times 10^{-9}$**

Table 10. The percentage of infectious viral particles (MPN) to the total number of viruses produced (VLP) for EhV -99B1, -208 and -86 propagated on host CCMP374. Burst-size represents number of VLPs released from each cell with standard error and is based on flow cytometric count.

EhV	MPN/mL	VLPs/mL	Percentage of infectious particles[1]	Burst-Size
99B1	$1{,}01 \times 10^{6}$	$3{,}16 \times 10^{8}$	0,32%	816 ± 55
208	$9{,}13 \times 10^{5}$	$1{,}54 \times 10^{8}$	0,59%	519 ± 92
86	$2{,}80 \times 10^{5}$	$8{,}26 \times 10^{7}$	0,34%	212 ± 30

[1] Calculated by dividing MPN/mL on VLPs/mL and multiplying with 100%

3.3 Mesocosm experiment

A bloom of nanoeukaryotic cells with high side scatter, presumably *E. huxleyi*, and both infectious EhV and EhV-like particles were detected during the mesocosm experiment (Figure 15 and 16). The bloom formed in both bags (2 and 4) around day 10 and was followed by a sudden decline at day 17 (Figure 15). A viral population of EhV-like-particles increased rapidly after the crash of *E. huxleyi*. Prior to the *E. huxleyi* bloom crash (< day 15) there was another virus population with similar flow cytometric signal. This, however, were determined not to be EhV by comparing the signals with EhV in cultures, as the signals were slightly different (Larsen, NORCE, Norway, pers. commun.).

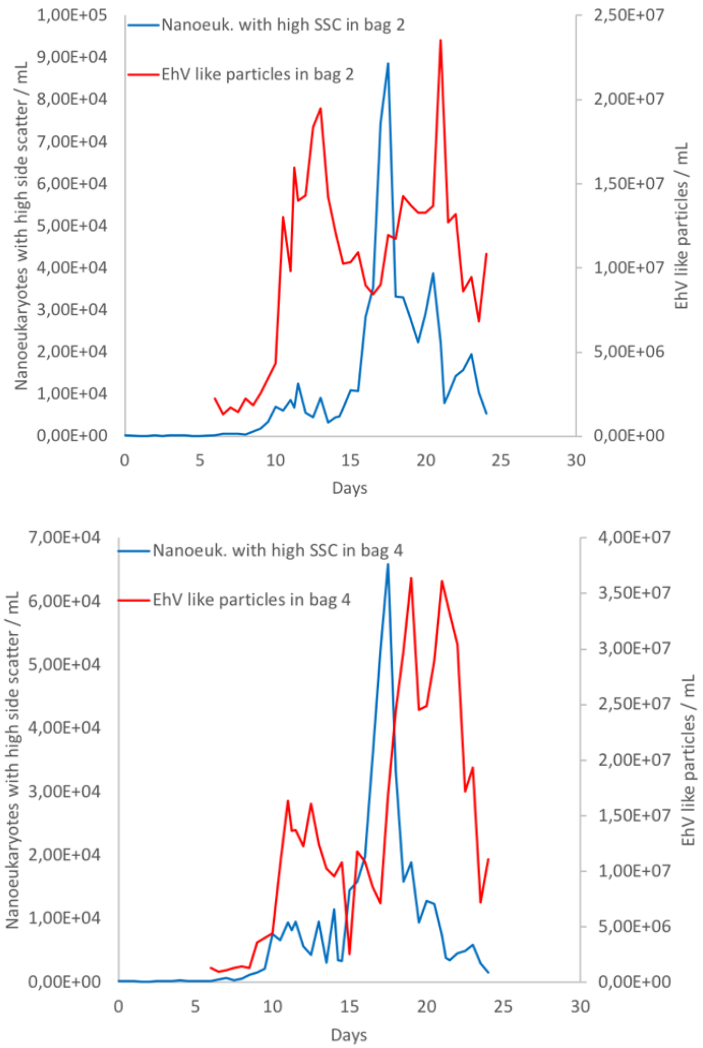

Figure 15. Flow cytometry count of EhV like particles and nanoeukaryotes with high side scatter (SSC) in the two mesocosm bags 2 (upper graph) and 4 (lower graph) during the experiment. Flow cytometry count data were obtained from Flora Vincent (Vardi Group – Weissman Institute).

3.3.1 Number of infectious particles (MPN)

Of the three host strains tested, infectious particles were only detected towards host strain CCMP374 during the mesocosm experiment (Figure 16). The first detected infectious particles appeared at day 12 in MPN-plate containing filtered sample water from bag 4 (8.7 MPN/mL). The MPN from this bag increased at day 16 and 18 (7.7×10^3 and 6.1×10^5 MPN/mL, respectively). A peak in MPN was reached at day 20 (1.2×10^6 MPN/mL) followed by a decrease at day 22 (2.4×10^5 MPN/mL). In bag 2 the first detected infectious particles appeared at day 16 with a concentration of 4.2×10^2 MPN/mL and increased to 9.4×10^3 MPN/mL at day 18. Both the peak and the MPN decline appeared the same days as in bag 4 (day 20 and 22), but with lower concentrations (1.7 and 1.2×10^5 MPN/mL, respectively).

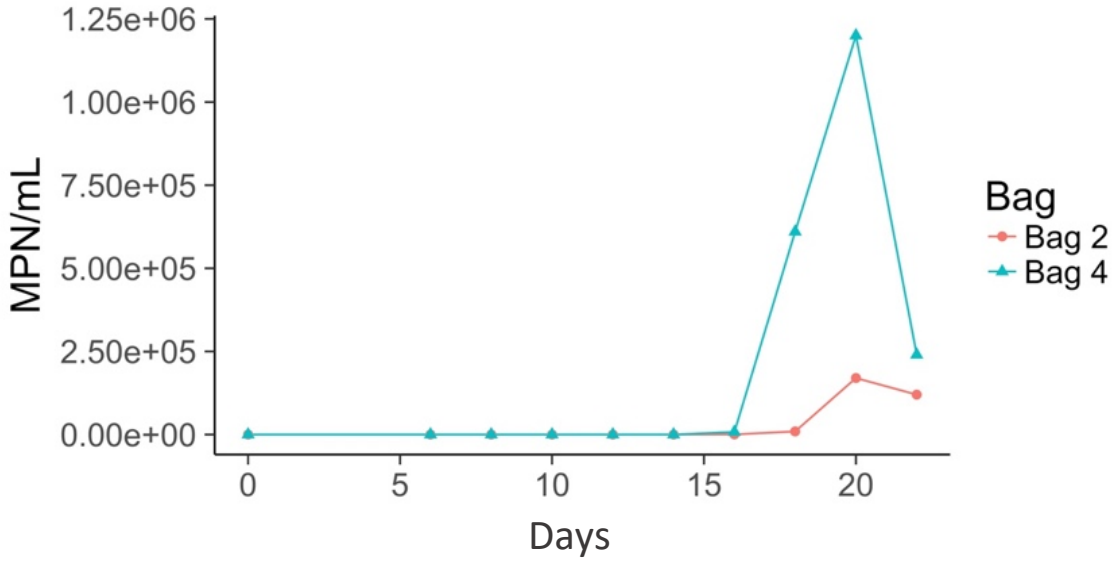

Figure 16. MPN concentrations from mesocosm bags 2 (circular points, red line) and 4 (triangular points, blue line) on host CCMP374 during the mesocosm experiment (non-logarithmic scale).

The virus particles present in the mesocosm bags did not propagate on the other two host strains (CCMP371 and B). However, a pattern was observed in the *in situ* relative fluorescence on these MPN plates.

The average relative fluorescence on MPN plates containing host culture CCMP371 in the column added undiluted sample (3^0) from mesocosm bag 2 (Figure 17, upper graph), varied between the three sampling days 18, 20 and 22. However, there was still a noticeable steep increase in average relative fluorescence up to dilution 3^{-4}, 3^{-3} and 3^{-5} with samples from days 18, 20 and 22, respectively. This increase was most prominent in serially diluted sample from day 22 of mesocosm bag 2.

On the MPN plates with the same host (CCMP371) added serially diluted sample from bag 2 (Figure 17, middle graph), had a low average relative fluorescence in the columns added undiluted (3^0) sample from all three days. A steep increase followed in the next dilutions, where samples from day 20 and 22 stagnated in average relative fluorescence at dilutions 3^{-3} and 3^{-2}, respectively. Sample from day 18 had a further steady increase until dilution 3^{-6} before the increased stagnated.

The MPN plates containing host strain B (Figure 17, lower graph) with sample from day 18 and 22 of bag 4 had a steady increase in average relative fluorescence until dilutions 3^{-6} and 3^{-4}, respectively. Sample from day 20 of this bag, had a steady increase throughout the whole dilution series. Sample from day 22 in bag 2 had a steep increase in average relative fluorescence until dilution 3^{-5}, before stagnating. MPN data with samples from day 18 and 20 (bag 2) are not included in this figure as there were no noticeable patterns from these samples. The Figure C-4 in Appendix C.3 show examples of how the graphs are expected to look like if the host (CCMP374) are added a virus that can propagate and produce infectious particles (data from the mesocosm).

The percentage of infectious particles in Table 11, was initial 0.08 and 0.07%, but increased to a peak with 1.28 and 4.28 % at day 20 in bags 2 and 4, respectively. Samples from bag 4 had an overall higher percentage of infectious EhV particles compared to bag 2 with higher concentrations of both EhV-like particles and MPN.

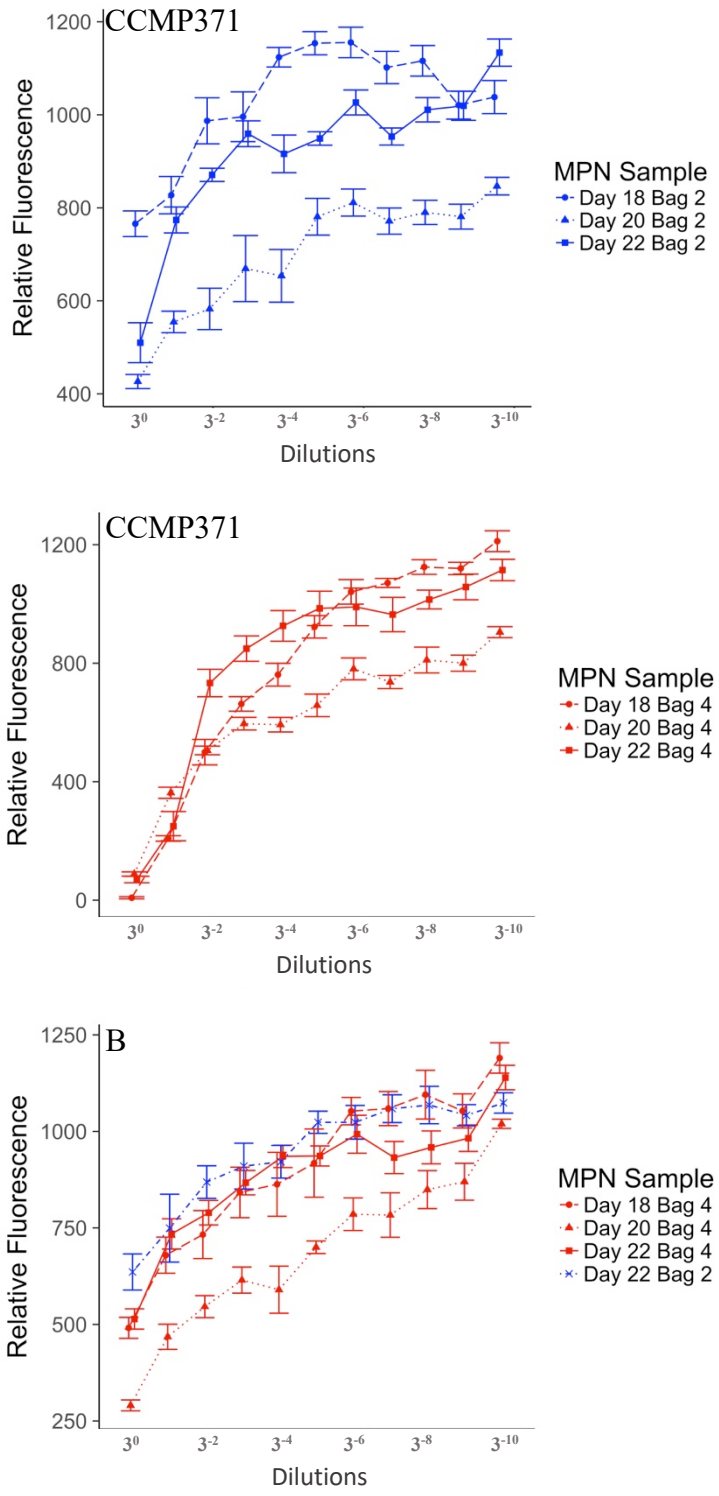

Figure 17. The graphs show the average *in situ* relative fluorescence for strains CCMP371 and B on MPN plates added filtered sample water from mesocosm bags 2 (in blue) and 4 (in red) from day 18 (circular points, solid lines), 20 (triangular points, dotted lines) and 22 (squared points, dashed lines). Each value on the x-axis represent the average relative fluorescence of all eight wells in a column of the MPN plates with standard error bar. The data points have been dodged (x-axis) in order to separate them where there is overlap.

Table 11. The percentage of infectious viral particles (MPN) of the total number of EhV-like particles (VLPs) measured during mesocosm experiment on host strain CCMP374. VLPs were estimated using Flow Cytometer by Flora Vincent from the Vardi Group.

Days	Bag	MPN/mL	VLPs/mL	Percentage of infectious particles[1]
18	2	$9{,}40 \times 10^{3}$	$1{,}17 \times 10^{7}$	0,08%
20	2	$1{,}70 \times 10^{5}$	$1{,}33 \times 10^{7}$	1,28%
22	2	$1{,}20 \times 10^{5}$	$1{,}32 \times 10^{7}$	0,91%
16	4	$7{,}70 \times 10^{3}$	$1{,}08 \times 10^{7}$	0,07%
18	4	$6{,}10 \times 10^{5}$	$2{,}45 \times 10^{7}$	2,49%
20	4	$1{,}20 \times 10^{6}$	$2{,}48 \times 10^{7}$	4,83%
22	4	$2{,}40 \times 10^{5}$	$3{,}04 \times 10^{7}$	0,79%

[1] Calculated by dividing MPN/mL on VLPs/mL and multiplying with 100%

3.3.2 EhV diversity during the mesocosm bloom

The four isolated virus strain from the mesocosm (2.4.3) that were cloned and sequenced using *mcp* gene (2.4.6), showed high homology when aligned and there were only nucleotide variations present at the ends (Appendix C.4, Alignment C-1). Excluding these nucleotide variations, the sequences are completely homolog to the OTU (Operational Taxonomic Unit; OTU 1) of the Illumina sequences that was dominant in all samples from days 12, 16, 20 and 22 (Appendix C.5, Table C-1). The other OTUs found in lower abundances (OTU 2-5) had only 1 nucleotide difference at various loci (single nucleotide polymorphism, SNP), but otherwise homolog to the most abundant OTU 1 (Appendix C.5, Alignment C-2).

The phylogenetic analysis of *mcp* shown in Figure 18 produced two main clusters (I and II). All OTUs and the isolated EhVs from the present study grouped into cluster (II), where they form a distinct clade with bootstrap value of 89%, most closely related to two other clades (79% bootstrap value) consisting of the EhV strains 18, 156, and 203 (98% bootstrap value), and 201 and 205 (94% bootstrap value). In group I there were two subgroups (69 and 94% bootstrap value) both consisting of environmental OTUs and isolated EhV strains.

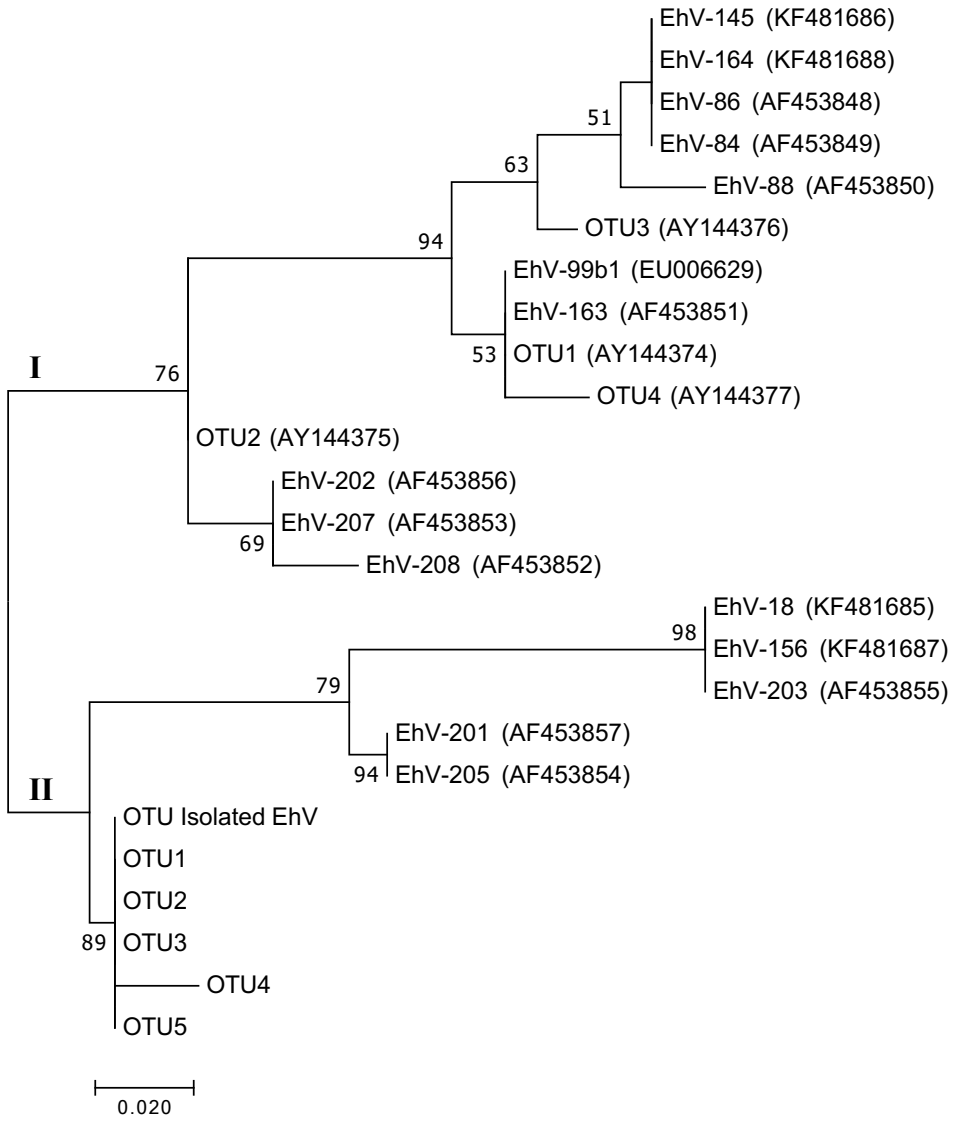

Figure 18. Phylogenetic reference tree constructed using Maximum Likelihood based on the Tamura-Nei model with 500 bootstrap replications. Bootstrap values <50% has been disregarded. OTU isolated EhV and OTU 1-5 are the most prominent in the mesocosm study. The other OTUs are collected from a previous mesocosm study in 2000 and 2003 from the same fjord (Martinez et al., 2007). GenBank accession number are included for sequenced OTUs and isolates.

4 Discussion

4.1 Are there significant variations in infectious patterns between virus and host at the strain level and does it reflect upon the virus having generalistic or specialistic properties?

4.1.1 Variations in infectious patterns

Similar infection patterns were observed for the host strains CCMP374, CCMP371 and B when infected with EhV-99B1 with a decrease in the infected host cell number followed by a sharp increase in the virus number (Figure 9). However, host strain B produced twice the number of infectious particles (2 x 10^6 MPN/mL) compared to the two other strains (both 1 x 10^6 MPN/mL; Figure 10). We also observed host strain B had a higher MPN towards EhV-99B1 when testing the initial EhV-99B1 lysate (3.2.1) used in the setup of the cross-infection experiment. Despite all three host MPN plates being inoculated with the same serially diluted EhV-99B1 lysate, and thus the same number of virus particles, host strain B produced the highest number of infectious particles (9.8x10^5 MPN/mL) compared to host strain CCMP374 and CCMP371 (4.7 and 6.1x10^5 MPN/mL, respectively). A possible explanation for this is that both EhV-99B1 and host strain B were isolated from Raunefjorden, and may thus have coevolved, making host strain B a more suitable host for this EhV strain. A similar result was obtained by Sahlsten (1998), where virus samples produced the highest MPN when using an algal strain isolated from the same region as the virus. It is however important to keep in mind that the host and virus strain in this study were isolated separately (1991 and 1999) and have been maintained in cultures over a long period of time. It has also been shown that dominating EhV strains terminating blooms in mesocosms seem to differ in each experiment, making it less likely for isolated EhV-99B1 and host strain B to have encountered, due to the rapid change in viral dynamics (Allen et al., 2007; Martinez et al., 2007; Rowe et al., 2011). As EhV-99B1 was able to infect host strains CCMP374 and CCMP371 that are isolated at separate locations in the north Atlantic Ocean, we confirmed previous literature documenting that several EhV strains are able to infect hosts isolated at large spatio-temporal scales (Allen et al., 2007; Ruiz et al., 2017).

When comparing the total production of virus particles (VLPs), the observed pattern was different. EhV-99B1 produced approximately twice the number of VLPs on strain CCMP374 (3.2 x 10^8 VLPs/mL) compared to CCMP371 and B (1.5 and 1.7 x 10^8 VLPs/mL,

respectively) and only a low proportion of these virus particle were infectious (0.32%, 0.68% and 1.20% in CCMP374, CCMP371 and B cultures, respectively, Table 8). This is consistent with other studies that also have reported low percentages of infectious particles in algal viruses (~1 – 50%; Cottrell and Suttle, 1995; Dimmock et al., 2016; Klasse, 2015; Short, 2012; Van Etten et al., 1983b). A high production of defective particles is an explanation for the low number of infectious units. Defective particles usually have mutations or incomplete copies of the viral genome that results in one or more necessary products not being successfully encoded (Dimmock et al., 2016).

Despite having the lowest percentage of infectious particles, EhV-99B1 amplified on CCMP374 had the highest burst-size (816 ± 55 VLPs/cell), which was considerably higher than of strains CCMP371 and B (419 ± 92 and 491 ± 30 VLPs/cell, respectively). However, some factors such as absorption coefficient and viral burst size depend strongly on host traits (Short, 2012), especially for *E. huxleyi.* This algae has great adaptive capabilities and a high phenotypic plasticity, which could explain why we observed host strains responding differently to viral infection (Hagino et al., 2011; Kegel et al., 2013; Medlin et al., 1996; Young and Westbroek, 1991). It should also be considered that these host strains were isolated at separate geographical locations and have probably been subjected to different selective pressures in terms of virus activity, grazing and nutrient competition, which might be another reason for why they respond differently to virus infection.

A disparity in the cross-infection experiment was that the EhV-99B1 viral population gated lower on the green fluorescence y-axis scale in the flow cytometric scatter plot when propagated on host B, compared to host CCMP374 or CCMP371 (Appendix C.2, Figure C-3). The fluorescent stain used (SYBR Green I), targets DNA and its location on the fluorescence y-axis scale corresponds to the concentration of DNA within the particle or cell (Zipper et al., 2004). For instance, bacterial populations naturally gate higher on the fluorescent y-axis compared to EhV because of its larger DNA content (Giovannoni et al., 2005; Van Etten et al., 2002; Wilson et al., 2011). The shift in flow cytometric gating may indicate loss of DNA-sequences from the viral genome when EhV-99B1 propagates on host strain B. The lost sequences are likely non-essential as there was still a production of infectious particles. The viral sequences also had to be lost in a sufficient proportion of the infected cells and be of a certain size in order for this shift to be observable in the flow cytometric gating. A pulsed field gel electrophoresis (PFGE) would have confirmed and quantified this loss in the genome

(Schwartz and Cantor, 1984). Pagarete et al. (2014) reported that the gene content between several EhV strains varied, suggesting that viral genes might be lost or gained over time, a possible scenario in our study. However, genomic analysis is necessary to confirm our assumptions.

The cross-infection of both EhV -208 and -86 on the three host strains produced a similar infection pattern (Figure 11 and 12), where both virus strains were able to infect and propagate on CCMP374, but not CCMP371 or B. There was no visible production of virus particles in virus treated CCMP371 and B cultures implying that they are both resistant strains towards EhV -208 and -86. However, compared to control cultures there was a reduction in growth rates in both host strains with the addition of virus, being most pronounced with EhV-86. The same trend was also observed on the MPN plates added with initial EhV-208 and -86 lysate used to infect the cultures in the cross-infection experiment. The average *in situ* relative fluorescence of all the wells in a column appeared to be lowest where undiluted virus lysate was added, and rapidly increase down the dilution series (Figure 13). The same pattern also appeared on the MPN plates using the phylogenetically distinct EhV strains from the mesocosm experiment (Figure 17 and 18).

The reduction in growth may suggest that there is an interfering agent from the virus lysate that is non-replicative and inhibits the host cell growth for a short time. Viral enhanced extracellular vesicles (EVs), a signal molecule that has been shown to increase the infection dynamics in infected cultures (Schatz et al., 2017), is one possible reason for the reduced growth of CCMP371 and B when treated with EhV -208, -86 or EhV from the mesocosm. It might be that EVs, which are brought along in the lysate from the previous infection, initiates a defensive mechanism in the host cells that causes them to temporarily stop or slow the growth. Once these signaling molecules are all either absorbed or impaired by natural degradation, the growth of the host resumes.

Another possible explanation is that the virus particles themselves inhibit the growth of CCMP371 and B. Viral encoded glycosphingolipids, which are enriched in the membrane of the virus particles, have signaling properties that can induce programmed cell death (PCD; Vardi et al., 2009). The question is, why are not more cells affected when there was a much higher number of virus particles compared to host cells (MOIs 5.31 and 10.63 for EhV -208 and -86, respectively)? Overall, we measured only a low percentage of infectious units to total

virus particles (<1.20%). It is therefore possible that only a low number of infectious particles are required to induce PCD and that altruistic kin-selection made the proportion of infected host cells spare the rest of the population from viral attack (Refardt et al., 2013; Shub, 1994). It could also be that genetic variability in the host cultures develops as a result of being cultivated for a long time, making some cell lines susceptible to infection. In order to observe host-virus response in the absence of genetic variability, we could have prepared clonal cultures (Blanco-Ameijeiras et al., 2016; Kegel et al., 2013).

Ruiz et al. (2017) demonstrated that both EhV -208 and -86 were able to infect and produce virus particles on CCMP371 and B, which contradicts with our results. In a separate cross-infection study (data not shown), we were also able to confirm that EhV-208 caused a significant reduction in cell number on CCMP371 (from 1.76 x 10^5 cells/mL at day 0 to 1.96 x 10^4 cells/mL at day 3 with virus treatment), however, we could not confirm lysis on host strain B, or that EhV-86 could lyse any of these host strains. Recent experiments, (Lawrence, UNB, Canada, pers. commun.) indicate that several EhV strains are not always able to cause a culture to crash over multiple rounds of infection. Some EhV strains are only able to induce a culture crash once, suggesting that either no or few infectious particles are being produced (dead-end host). Since the production of infectious particles were not considered in the study of Ruiz et al. (2017), we cannot verify that CCMP371 or B are true hosts of EhV -208 and -86.

On the other hand, assuming that EhV -208 and -86 produced infectious particles on CCMP371 and B in Ruiz et al. (2017), it is possible that these virus strains have lost necessary mechanisms for successful infection after being propagated on a different host (CCMP374) over multiple rounds (>7). Since the EhV strains consequently encountered CCMP374, mutations or loss in genes encoding necessary attachment proteins targeting CCMP371 or B, would not have had a directly negative impact on the viruses. It is also possible that EhV-99B1 naturally has a broader host range compared to EhV -208 and -86, as it has a different genetic composition, where EhV-99B1 contains a subset of genes that is lacking in EhV -208 and -86 and vice versa (Pagarete et al., 2014). The genetic similarity between EhV -208 and -86 (Pagarete et al., 2014) and similar infection patterns are consistent with them both being isolated from the same region (English Channel). It is also coherent that EhV-99B1, which has both a different gene composition and infectious pattern than of EhV -

208 and -86, was isolated in a geographically separated region (Raunefjorden; Appendix A, Table A-2).

Considering these infections from the host perspective, our study indicates that CCMP371 and B are more resistant to EhVs compared with CCMP374, as this strain was successfully infected by all three virus strains. The dominant viral OTU from the mesocosm experiment was phylogenetically distinct from EhV-208 and -86 (Figure 18), but exploited the same infectious pattern, which further supports that CCMP374 are more susceptible to a broader range of viruses compared to CCMP371 and B. In this study we did not focus upon host traits, but several studies have documented a cost of resistance (e.g. lower growth rate) to parasite or virus infection (Benmayor et al., 2008; Brockhurst et al., 2005, 2004; Gómez and Buckling, 2011; Middelboe et al., 2009). Nonetheless, we did observe that host strain CCMP374 cultures reached denser cell abundances prior to stationary phase and that it maintained better growth under high light intensity on MPN plates, compared to CCMP371 and B (data not shown). These features might make CCMP374 more competitive compared to other strains or species, but with the cost of having poor resistance mechanisms towards infection.

Another interesting observation in the cross-infection experiments was that the final yield of virus particles appeared around day 2, but the host cells still decreased after this measurement (day 3). Brussaard (2004) documented that infected algal cultures of *Phaeocystis pouchetii* declined in number of live cells a few hours before cell number declined. As EhV acquires their external envelope by budding through the host plasma membrane (Mackinder et al., 2009), it is possible that the virus particles were released from the host cell without disrupting the cell membrane. The host cell will eventually die as viruses usually promotes PCD in some way. They can for instance interfere with host machinery (e.g. inhibiting photosynthetic machinery), which may lead to starvation of the cell that will burst the cell (Dimmock et al., 2016; Juneau et al., 2003). It is quite possible that this is the reason for why we observed a lag between virus release and host cell death in our study.

4.1.2 Generalist or specialist virus

EhV-99B1 was the only virus strain in this study that was able to produce infectious particles on all three host strains (CCMP374, CCMP371 and B). Being able to infect several hosts, suggests that this virus strain has generalistic properties. EhV -208 and -86 on the other hand,

were only able to infect one host strain (CCMP374), which suggests specialistic properties. We would expect to see trade-offs for being a generalist, as this is a costly feature (Gómez and Buckling, 2011; Keen, 2014), but on the contrary the specialists did not present any obvious benefits over the generalist. The specialist EhV-86 produced both less infectious (2.8 x 10^5 MPN/mL) and total virus particles (8.3 x 10^7 VLPs/mL) compared to the generalist EhV-99B1 (1.0 x 10^6 MPN/mL and 3.2 x 10^8 VLPs/mL; Figure 14). The specialist EhV-208 however, had a slight benefit in having somewhat higher percentage of infectious particles to total virus particles (0.59%) compared to EhV-99B1 (0.39%). However, it is possible that the specialistic viruses have been affected by being cultivated over a long period of time (>18 years), causing them to gradually lose infectivity.

A previous *E.huxleyi*-EhV cross-infection study also observed that specialist viruses did not exploit much benefits over generalists when comparing virus particle production (Ruiz et al., 2017). Further it has been demonstrated that a generalist (EhV-207) can quickly outcompete a specialist virus (EhV-86; Nissimov et al., 2016). These results combined with the results from our study, means that for a specialist virus to coexist with generalist viruses and not be outcompeted in the marine environment, there have to be other trade-offs (e.g. decay rate).

Nevertheless, if we consider host traits our data is more consistent with 'killing the winner' dynamics (KtW; Thingstad, 2000; Thingstad et al., 2014; Våge et al., 2016). Host strain CCMP374 seem to display better growth properties compared to CCMP371 or B, but CCMP374 was also the most susceptible host as well, being infected by both the generalist (EhV-99B1) and the specialist viruses (EhV -208, -86 and mesocosm EhV). The two other host strains CCMP371 and B, presumably defense specialists, were only infected by the generalist EhV-99B1. These host trade-offs in being a defense specialist or a growth competitor might be the reason for why such different life-strategies can coexist (Figure 2).

4.2 Will the infectious pattern vary between host strains when infected with EhV particles from a mesocosm study?

Infecting our three host strains with samples from a mesocosm experiment displayed lysis only on host strain CCMP374. There was one EhV genotype detected throughout the bloom and we classified it as an acute specialist virus as it spread rapidly and had a narrow host range. These features might be consistent with the expected trade-offs in KtW model, where

the EhV from the mesocosm was able to quickly terminate a bloom but with the cost of having a narrow host range. However, we should be cautious with concluding that the mesocosm EhV strain is a specialist virus, as it possible that our three tested host strains are not a representative host range. Studies typically report a decline in EhV diversity as the virus population increases in blooming scenarios (Martinez et al., 2007; Schroeder et al., 2003; Sorensen et al., 2009), however, we measured only one EhV genotype throughout the bloom (with a few less abundant SNP variants; Appendix C.5), but it is possible that we could have measured the same decline in viral diversity if we had carried out Illumina sequencing on mesocosm samples from earlier in the bloom.

The infectious growth pattern within the two mesocosm bags displayed similar patterns with both bags peaking in infectious particles at day 20 (Figure 16). Bag 4, however, had a considerable higher peak of both infectious and total virus particles (1.2 x 10^6 MPN/mL and 2.5 x 10^7 VLPs/mL) compared to bag 2 (1.7 x 10^5 MPN/mL and 1.3 x 10^7 VLPs/mL). As bag 4 also had a lower peak of *E. huxleyi* cells (6.6 x 10^4 cells/mL) compared to bag 2 (8.9 x 10^4 cells/mL) it may indicate that the host cells in bag 4 produced higher viral burst sizes, compared to the host cells in bag 2. Since the EhV genetic composition was similar in both bags (Appendix C.5, Table C-1), based on the *mcp* gene similarities, it is possible that the *E. huxleyi* genetic composition differed between these bags. The host cells in bag 4 might have had a higher number of susceptible cells compared to the cells of bag 2, resulting in an overall higher EhV concentration. Unfortunately, the genetic host composition was not monitored, so we can only speculate if this was the case.

4.3 To what extent is the viral burst sizes affected by MOI?

In order to find the minimum multiplicity of infection (MOI) needed to produce a one-step growth curve, we tested several relative MOI-concentrations (Figure 7). Brown and Bidle (2014) documented that the mean burst sizes were significantly diminished with increasing MOI using the *Aureococcus anophagefferens*-Brown Tide virus (AaV) system. We observed a similar result, where the burst sizes diminished with increasing relative MOI-concentration, and regardless of the initial MOI, the final number of virus particles were consequently the same (EhV -99B1: 1.7-2.3 x 10^8, EhV-208: 1.1-1.9 x 10^8 and EhV-86: 1.2-1.7 x 10^8 VLPs/mL). This suggests that there is a negative feedback mechanism that causes the burst sizes to decrease with increasing MOIs.

In Brown and Bidle (2014) this phenomenon was explained by 'lysis from without', which is classically caused by multiple punctures on the cell membrane by lysozyme activity during absorption, and thus stopping the production of new virus particles. Since EhV exploit an animal like infection, where they enter by an enveloped fusion mechanism or endocytosis (Mackinder et al., 2009), it is possible that when multiple EhV particles attach to the host cell-membrane it loses its integrity and burst before any viral multiplication. This is further confirmed by our observations in Figure 7, where the cells died faster with increasing relative MOI-concentrations, already after 24 hours, a time when virus induced cell death is minimal (Schatz et al., 2017).

Another explanation for this phenomenon might be the presence and production of viral enhanced extracellular vesicles (EV). Production of EVs are dose-dependent (high dose yields high production) and can be detected in high abundances in infected cultures already by 24 hours (Schatz et al., 2017). It is therefore possible that the EVs are the cause behind the rapid cell death and the controlled virus yield as seen in our study. We can assume that with an increasing MOI there will be more EVs added initially, which would further increase the production of EV in infected cells and terminate the production of new virus particles in a larger number of cells. With such a negative feedback mechanism the burst sizes should be constant, regardless of the initial MOI, where it is only the concentration and the dose-dependent production of EV that controls the number of cells that are able to produce new virus particles.

If EVs can induce programmed cell death it might also explain the inadequate presence of infectious particles. For instance, a one-step growth curve was achieved using an MOI of 1.26 virus particles per host cell with EhV-99b1, but in the cross-infection we measured that only 0.32% of the total virus particles were infectious on CCMP374. This means that the infectious MOI was only 0.004 and yet the culture crashed. The presence and further production of EVs might explain why the culture crashed, despite the insufficient number of infectious particles.

4.4 Discussion of methods

4.4.1 Defining the minimum MOI that maintains a one-step growth curve

Our method for finding the minimum MOI was mainly based on the visual observation of the growth curve of the infected cultures, meaning our results could be inaccurate. A better indication of the minimum MOI would have been achieved if we had monitored the infected cultures further. Longer incubations would have likely presented a two-step growth curve in cultures with insufficient number of virus particles to infect every cell (too low MOI) and we could have chosen a slightly higher MOI based on this (Flint et al., 2015).

Ellis and Delbrück (1939) explained another method to ensure one-step growth without excess virus particles. They infected bacterial cells at MOIs of 10 infectious phage particles per host cell, to ensure infection of every cell in the culture. Then, after allowing enough time for the phage particles to attach (5 min), they centrifuged the culture to a pellet of cells and their attached phages. The supernatant containing unattached phage particles was discarded and replaced with fresh medium, providing an infected cell culture with low numbers of free phage particles. However, dealing with eukaryotic cells as in this study, the centrifugation step would likely have damaged the cells (Peterson et al., 2012).

4.4.2 Most Probable Number (MPN)

As the proportion of infectious particles was much lower than the total viral particle count (<1.20%), we verified a subset of MPN results to confirm that the values estimated by the MPN software were correct. We illustrate this with an MPN plate containing host strain CCMP374 added with serially diluted EhV-99B1 (~ 4 x 10^8 VLPs/mL, undiluted virus concentration). In this MPN plate there was lysis in three out of the eight wells at the 5^{-6} dilution, suggesting there were at least three infectious particles per eight well. As we added 0.01 mL serially diluted sample in each of the eight wells, it means there should have been three infectious particles per 0.8 mL or 0.375 infectious particle per 0.1 mL. However, if we calculate how many virus particles there should be in each well of this dilution, we obtain a much higher value: 4 x 10^8 VLPs/mL x 5^{-6} dilution x 0.01 mL = 256 VLPs. Our theoretical calculations suggest there should have been approximately 256 VLPs per 0.01 mL at 5^{-6} dilution, but only 3 out of 8 wells lysed. If we multiply this probability (3/8) with the

theoretically added VLPs (256), it suggests there was only 1 infectious unit per 96 virus particles, which is quite close to the calculated percentages of infectious particles (0.34-1.20%). This example provides higher confidence that the calculations from the MPN software are indeed correct.

Conclusion

The three EhV and *E. huxleyi* strains used in the cross-infection informed us that differences in infectious pattern appear even in narrow phylogenetic spectrums. EhV-99B1 was the only virus strain of the three to successfully propagate on the three host strains CCMP374, CCMP371 and B. There were differences in infectious and virus particle production, where infected strain B had twice the production of infectious particles compared to strains CCMP374 and CCMP371. On the other hand, the infected CCMP374 strain produced roughly twice the number of total virus particles compared to strains CCMP371 and B. The two other virus strains, EhV -208 and -86, were only able to propagate on host CCMP374, but did cause a reduction in growth on CCMP371 and B. These two EhV strains were in this study classified as specialist viruses due to their narrow host range, however, in terms of infectious and total virus particle production they did not present any notable beneficial traits that exceeded the generalist EhV-99B1.

There was one dominating EhV genotype that was present throughout the bloom of the mesocosm. This EhV strain was determined to be an acute specialist virus as it spread rapidly and was only able to propagate on CCMP374. However, it did cause a reduction in growth on CCMP371 and B, similar to the effect of EhV -208 and -86. This illustrated that variations do occur between host strains when infected with EhV particles from a natural community and that it presents similar patterns to that of cultured virus strains. As the mesocosm OTU was phylogenetically distinct from EhV -99b1, -208 and -86 it furthermore supported our assumptions that CCMP371 and B are defense specialists and CCMP374 are a competition specialist as indicated by their growth properties. These host traits may fit the trade-offs that are expected in kill the winner dynamics.

The burst sizes diminished with increasing relative MOI concentrations, in such a manner that the final number of viruses was consequently the same, regardless of the initial MOI. We proposed viral enhanced extracellular vesicles as the causative agent for this negative feedback mechanism.

Future work

The variability in infectious patterns between a few strains of *E. huxleyi* and their viruses shown in our study indicates how diverse these systems are, and how much is yet to be learned. Cross-infection studies will help us gain further understanding of how these systems function and explore the diversity of virus-host interactions. It is of great ecological interest to investigate how and when specific viruses can or cannot infect algal hosts, which is why it is necessary to investigate these interactions further. I propose investigating both bloom and non-bloom forming phytoplankton representatives and compare these different lifestyles in terms of infectious pattern. I also propose comparing the phylogeny of both the viruses and the host, to see if they group together in terms of evolutionary traits.

In a pilot cross-infection study (data not shown), I used a local *E. huxleyi* host strain named BOF. However, I could not continue to use this strain as it did not give definite results in the MPN method, which were an important part of our study. The BOF strain displayed good growth on the MPN plates, but I discovered that it produced a different number of infectious particles depending on the host starting cell density. For instance, a low starting density revealed a high proportion of infectious virus particles and vice versa. The BOF host strain contains properties not found in the other three strains CCMP374, CCMP371 and B, and in terms of infection dynamics, it would have been interesting to further investigate this evolutionary trait.

I proposed extracellular vesicles (EV) as the causative agent for the reduced growth with increasing MOI and as the negative feedback mechanism in virus production. However, it is necessary to confirm these assumptions and further explore the function of EVs during infection. One way of testing our assumptions is to create a virus free lysate that only contains EVs and see if they can reduce the growth on our host strains. As bacteria, archaea, metazoans and other protists also naturally produce EVs, it should be investigated if the phenomenon found in the EhV-*E. huxleyi* systems also occur in other groups as well.

Coevolution between most virus-host system occurs rapidly, and it would have an interesting aspect to investigate the rates of these evolutionary changes. This could have been tested by simply propagating a virus strain on the same host strain over multiple rounds of infection.

The genetic composition and the production of both infectious and total virus particles could then have been monitored, to observe how these factors change over time.

Another parameter to include in the cross-infection experiment is to investigate the production of empty virions. Empty virions cannot be detected using the flow cytometer, as the stain targets the viral DNA for enumeration. A cesium chloride density gradient assay and quantification by nanodrop would have allowed us to investigate the production of empty virions and observe if this is a factor that varies between EhV strains.

Understanding the extracellular vesicles (EVs) from the *E. huxleyi* – EhV system could provide an insight into the biotechnological applications of this algal system. EVs have already been proposed as a biotechnological tool for treating different diseases (Crenshaw et al., 2018; Rodrigues et al., 2018). A promising area is the use of EVs in treating brain cancer as it potentially can cross the blood brain barrier (Ciregia et al., 2017). This can possibly allow us to use genetically modified viruses that infects mammalian cells as a tool to produce EVs that can target specific cancer cells in vivo.

References:

Ackleson, S., Balch, W., Holligan, 1988. White Waters of the Gulf of Maine. Oceanography 1, 18–22. https://doi.org/10.5670/oceanog.1988.03

Allen, M.J., Martinez-Martinez, J., Schroeder, D.C., Somerfield, P.J., Wilson, W.H., 2007. Use of microarrays to assess viral diversity: from genotype to phenotype. Environmental Microbiology 9, 971–982. https://doi.org/10.1111/j.1462-2920.2006.01219.x

Azam, F., Fenchel, T., Field, J., Gray, J., Meyer-Reil, L., Thingstad, F., 1983. The Ecological Role of Water-Column Microbes in the Sea. Marine Ecology Progress Series 10, 257–263. https://doi.org/10.3354/meps010257

Benmayor, R., Buckling, A., Bonsall, M.B., Brockhurst, M.A., Hodgson, D.J., 2008. The interactive effects of parasites, disturbance, and productivity on experimental adaptive radiations. Evolution 62, 467–477. https://doi.org/10.1111/j.1558-5646.2007.00268.x

Bergh, Ø., Børsheim, K.Y., Bratbak, G., Heldal, M., 1989. High abundance of viruses found in aquatic environments. Nature 340, 467–468. https://doi.org/10.1038/340467a0

Bidle, K.D., 2016. Programmed Cell Death in Unicellular Phytoplankton. Current Biology 26, R594–R607. https://doi.org/10.1016/j.cub.2016.05.056

Blanco-Ameijeiras, S., Lebrato, M., Stoll, H.M., Iglesias-Rodriguez, D., Müller, M.N., Méndez-Vicente, A., Oschlies, A., 2016. Phenotypic Variability in the Coccolithophore *Emiliania huxleyi*. PLOS ONE 11, e0157697. https://doi.org/10.1371/journal.pone.0157697

Bongiorni, L., Magagnini, M., Armeni, M., Noble, R., Danovaro, R., 2005. Viral production, decay rates, and life strategies along a trophic gradient in the North Adriatic Sea. Applied and environmental microbiology 71, 6644–6650. https://doi.org/10.1128/AEM.71.11.6644-6650.2005

Bratbak, G., Egge, J.K., Heldal, M., 1993. Viral mortality of the marine alga *Emiliania huxleyi* (Haptophyceae) and termination of algal blooms. Marine Ecology Progress Series 93, 39–48. https://doi.org/10.3354/meps093039

Bratbak, G., Jacobsen, A., Heldal, M., Nagasaki, K., Thingstad, F., 1998. Virus production in *Phaeocystis pouchetii* and its relation to host cell growth and nutrition. Aquat. Microb. Ecol. 16, 1–9. https://doi.org/10.3354/ame016001

Bratbak, G., Thingstad, F., Heldal, M., 1994. Viruses and the microbial loop. Microbial Ecology 28, 209–221. https://doi.org/10.1007/BF00166811

Bratbak, G., Wilson, W., Heldal, M., 1996. Viral control of *Emiliania huxleyi* blooms? Journal of Marine Systems 9, 75–81. https://doi.org/10.1016/0924-7963(96)00018-8

Breitbart, M., 2012. Marine Viruses: Truth or Dare. Annual Review of Marine Science 4, 425–448. https://doi.org/10.1146/annurev-marine-120709-142805

Brockhurst, M.A., Buckling, A., Rainey, P.B., 2005. The effect of a bacteriophage on

diversification of the opportunistic bacterial pathogen, *Pseudomonas aeruginosa*. Proceedings. Biological sciences 272, 1385–1391. https://doi.org/10.1098/rspb.2005.3086

Brockhurst, M.A., Rainey, P.B., Buckling, A., 2004. The effect of spatial heterogeneity and parasites on the evolution of host diversity. Proceedings. Biological sciences 271, 107–111. https://doi.org/10.1098/rspb.2003.2556

Brown, C.M., Bidle, K.D., 2014. Attenuation of virus production at high multiplicities of infection in *Aureococcus anophagefferens*. Virology 466–467, 71–81. https://doi.org/10.1016/j.virol.2014.07.023

Brown, C.W., Yoder, J.A., 1994. Coccolithophorid blooms in the global ocean. Journal of Geophysical Research: Oceans 99, 7467–7482. https://doi.org/10.1029/93JC02156

Brown, L., Wolf, J.M., Prados-Rosales, R., Casadevall, A., 2015. Through the wall: extracellular vesicles in Gram-positive bacteria, mycobacteria and fungi. Nature Reviews Microbiology 13, 620. https://doi.org/10.1038/nrmicro3480

Brum, J.R., Sullivan, M.B., 2015. Rising to the challenge: accelerated pace of discovery transforms marine virology. Nature Reviews Microbiology 13, 147. https://doi.org/10.1038/nrmicro3404

Brussaard, C., Gast, G., van Duyl, F., Riegman, R., 1996a. Impact of phytoplankton bloom magnitude on a pelagic microbial food web. Marine Ecology Progress Series 144, 211–221. https://doi.org/10.3354/meps144211

Brussaard, C., Kempers, R., Kop, A., Riegman, R., Heldal, M., 1996b. Virus-like particles in a summer bloom of *Emiliania huxleyi* in the North Sea. Aquatic Microbial Ecology 10, 105–113. https://doi.org/10.3354/ame010105

Brussaard, C.P.D., 2004. Viral Control of Phytoplankton Populations - a Review. The Journal of Eukaryotic Microbiology 51, 125–138. https://doi.org/10.1111/j.1550-7408.2004.tb00537.x

Burkill, P.H., Archer, S.D., Robinson, C., Nightingale, P.D., Groom, S.B., Tarran, G.A., Zubkov, M.V., 2002. Dimethyl sulphide biogeochemistry within a coccolithophore bloom (DISCO): an overview. Deep Sea Research Part II: Topical Studies in Oceanography 49, 2863–2885. https://doi.org/10.1016/S0967-0645(02)00061-9

Castberg, T., Larsen, A., Sandaa, R., Brussaard, C., Egge, J., Heldal, M., Thyrhaug, R., van Hannen, E., Bratbak, G., 2001. Microbial population dynamics and diversity during a bloom of the marine coccolithophorid *Emiliania huxleyi* (Haptophyta). Marine Ecology Progress Series 221, 39–46. https://doi.org/10.3354/meps221039

Castberg, T., Thyrhaug, R., Larsen, A., Sandaa, R.-A., Heldal, M., Van Etten, J.L., Bratbak, G., 2002. Isolation and characterization of a virus that infects *Emiliania huxleyi* (Haptophyta). Journal of Phycology 38, 767–774. https://doi.org/10.1046/j.1529-8817.2002.02015.x

Ciregia, F., Urbani, A., Palmisano, G., 2017. Extracellular Vesicles in Brain Tumors and Neurodegenerative Diseases. Front Mol Neurosci 10, 276–276.

https://doi.org/10.3389/fnmol.2017.00276

Cottrell, M.T., Suttle, C.A., 1995. Dynamics of lytic virus infecting the photosynthetic marine picoflagellate *Micromonas pusilla*. Limnology and Oceanography 40, 730–739. https://doi.org/10.4319/lo.1995.40.4.0730

Cottrell, M.T., Suttle, C.A., 1991. Wide-spread occurrence and clonal variation in viruses which cause lysis of a cosmopolitan, eukaryotic marine phytoplankter, Micromonas pusilla. Marine Ecology Progress Series 78, 1–9. http://www.jstor.org/stable/24826998

Crenshaw, B.J., Gu, L., Sims, B., Matthews, Q.L., 2018. Exosome Biogenesis and Biological Function in Response to Viral Infections. Open Virol J 12, 134–148. https://doi.org/10.2174/1874357901812010134

Delbrück, M., 1940. The growth of bacteriophage and lysis of the host. J Gen Physiol 23, 643–660. https://doi.org/10.1085/jgp.23.5.643

Dimmock, N.J., Easton, A.J., Leppard, K.N., 2016. Introduction to Modern Virology, 7th ed. School of Life Sciences, University of Warwick, Coventry.

Dunigan, D.D., Fitzgerald, L.A., Van Etten, J.L., 2006. Phycodnaviruses: A peek at genetic diversity. Virus Research 117, 119–132. https://doi.org/10.1016/j.virusres.2006.01.024

Ellis, E.L., Delbrück, M., 1939. The growth of bacteriophage. The Journal of General Physiology 22, 365–384. https://doi.org/10.1085/jgp.22.3.365

Engelking, L.R., 2015. Sphingolipids, in: Engelking, L.R., Textbook of Veterinary Physiological Chemistry, 3rd ed. Academic Press, Boston, pp. 378–383. https://doi.org/10.1016/B978-0-12-391909-0.50059-1

Falkowski, P.G., 1994. The role of phytoplankton photosynthesis in global biogeochemical cycles. Photosynthesis Research 39, 235–258. https://doi.org/10.1007/BF00014586

Falkowski, P.G., Raven, J.A., 2007. An Introduction to Photosynthesis in Aquatic Systems, in: Aquatic Photosynthesis. Princeton University Press, pp. 1–43.

Fenchel, T., 2008. The microbial loop – 25 years later. Journal of Experimental Marine Biology and Ecology 366, 99–103. https://doi.org/10.1016/j.jembe.2008.07.013

Flint, J., Enquist, L., Racaniello, V., Rall, G., Skalka, A.M., 2015. Principles of virology, 4th ed. ASM Press, Washington D.C.

Fuhrman, J.A., 1999. Marine viruses and their biogeochemical and ecological effects. Nature 399, 541–548. https://doi.org/10.1038/21119

Fuhrman, J.A., Suttle, C.A., 1993. Viruses in Marine Planktonic Systems. Oceanography 6, 51–63. http://www.jstor.org/stable/43924641

Giovannoni, S.J., Tripp, H.J., Givan, S., Podar, M., Vergin, K.L., Baptista, D., Bibbs, L., Eads, J., Richardson, T.H., Noordewier, M., Rappé, M.S., Short, J.M., Carrington, J.C.,

Mathur, E.J., 2005. Genome Streamlining in a Cosmopolitan Oceanic Bacterium. Science 309, 1242. https://doi.org/10.1126/science.1114057

Gobler, C.J., Hutchins, D.A., Fisher, N.S., Cosper, E.M., Saňudo-Wilhelmy, S.A., 1997. Release and bioavailability of C, N, P Se, and Fe following viral lysis of a marine chrysophyte. Limnology and Oceanography 42, 1492–1504. https://doi.org/10.4319/lo.1997.42.7.1492

Gómez, P., Buckling, A., 2011. Bacteria-Phage Antagonistic Coevolution in Soil. Science 332, 106. https://doi.org/10.1126/science.1198767

Hagino, K., Bendif, E.M., Young, J.R., Kogame, K., Probert, I., Takano, Y., Horiguchi, T., de Vargas, C., Okada, H., 2011. New evidence for morphological and genetic variation in the cosmopolitan coccolithophore *Emiliania huxleyi* (Prymnesiophyceae) from the COX1b-ATP4 genes. Journal of Phycology 47, 1164–1176. https://doi.org/10.1111/j.1529-8817.2011.01053.x

Heldal, M., Bratbak, G., 1991. Production and decay of viruses in aquatic environments. Marine Ecology Progress Series 72, 205–212. https://doi.org/10.3354/meps072205

Hennes, K.P., Suttle, C.A., Chan, A.M., 1995. Fluorescently Labeled Virus Probes Show that Natural Virus Populations Can Control the Structure of Marine Microbial Communities. Appl Environ Microbiol 61, 3623–3627. https://aem.asm.org/content/61/10/3623.long

Highfield, A., Joint, I., Gilbert, J., Crawfurd, K., Schroeder, D., 2017. Change in *Emiliania huxleyi* Virus Assemblage Diversity but Not in Host Genetic Composition during an Ocean Acidification Mesocosm Experiment. Viruses 9, 41. https://doi.org/10.3390/v9030041

Holligan, P.M., Fernández, E., Aiken, J., Balch, W.M., Boyd, P., Burkill, P.H., Finch, M., Groom, S.B., Malin, G., Muller, K., Purdie, D.A., Robinson, C., Trees, C.C., Turner, S.M., van der Wal, P., 1993. A biogeochemical study of the coccolithophore, *Emiliania huxleyi*, in the North Atlantic. Global Biogeochemical Cycles 7, 879–900. https://doi.org/10.1029/93GB01731

Holligan, P.M., Groom, S.B., 1986. Phytoplankton distributions along the shelf break. Proceedings of the Royal Society of Edinburgh. Section B. Biological Sciences 88, 239–263. https://doi.org/10.1017/S0269727000004589

Hurwitz, B.L., Sullivan, M.B., 2013. The Pacific Ocean Virome (POV): A Marine Viral Metagenomic Dataset and Associated Protein Clusters for Quantitative Viral Ecology. PLOS ONE 8, e57355. https://doi.org/10.1371/journal.pone.0057355

Hutchinson, G.E., 1961. The Paradox of the Plankton. The American Naturalist 95, 137–145. http://www.jstor.org/stable/2458386

Jacquet, S., Heldal, M., Iglesias-Rodriguez, D., Larsen, A., Wilson, W., Bratbak, G., 2002. Flow cytometric analysis of an *Emiliana huxleyi* bloom terminated by viral infection. Aquat. Microb. Ecol. 27, 111–124. https://doi.org/10.1080/19475721003743843

Jacquet, S., Miki, T., Noble, R., Peduzzi, P., Wilhelm, S., 2010. Viruses in aquatic

ecosystems: important advancements of the last 20 years and prospects for the future in the field of microbial oceanography and limnology. Advances in Oceanography and Limnology 1, 97–141. https://doi.org/10.1080/19475721003743843

Jarvis, B., Wilrich, C., Wilrich, P.-T., 2010b. Reconsideration of the derivation of Most Probable Numbers, their standard deviations, confidence bounds and rarity values. Journal of Applied Microbiology 109, 1660–1667. https://doi.org/10.1111/j.1365-2672.2010.04792.x

Juneau, P., Lawrence, J., Suttle, C., Harrison, P., 2003. Effects of viral infection on photosynthetic processes in the bloom-forming alga *Heterosigma akashiwo*. Aquat. Microb. Ecol. 31, 9–17. https://doi.org/10.3354/ame031009

Keen, E.C., 2014. Tradeoffs in bacteriophage life histories. Bacteriophage 4, e28365. https://doi.org/10.4161/bact.28365

Kegel, J.U., John, U., Valentin, K., Frickenhaus, S., 2013. Genome variations associated with viral susceptibility and calcification in *Emiliania huxleyi*. PLOS ONE 8, e80684–e80684. https://doi.org/10.1371/journal.pone.0080684

Klasse, P.J., 2015. Chapter Ten - Molecular Determinants of the Ratio of Inert to Infectious Virus Particles, in: Progress in Molecular Biology and Translational Science. Academic Press, pp. 285–326. https://doi.org/10.1016/bs.pmbts.2014.10.012

Kulp, A., Kuehn, M.J., 2010. Biological Functions and Biogenesis of Secreted Bacterial Outer Membrane Vesicles. Annu. Rev. Microbiol. 64, 163–184. https://doi.org/10.1146/annurev.micro.091208.073413

Kumar, S., Stecher, G., Tamura, K., 2016. MEGA7: Molecular Evolutionary Genetics Analysis Version 7.0 for Bigger Datasets. Molecular Biology and Evolution 33, 1870–1874. https://doi.org/10.1093/molbev/msw054

Larsen, A., Castberg, T., Sandaa, R., Brussaard, C., Egge, J., Heldal, M., Paulino, A., Thyrhaug, R., van Hannen, E., Bratbak, G., 2001. Population dynamics and diversity of phytoplankton, bacteria and viruses in a seawater enclosure. Marine Ecology Progress Series 221, 47–57. https://doi.org/10.3354/meps221047

Liu, H., Probert, I., Uitz, J., Claustre, H., Aris-Brosou, S., Frada, M., Not, F., de Vargas, C., 2009. Extreme diversity in noncalcifying haptophytes explains a major pigment paradox in open oceans. Proc. Natl. Acad. Sci. USA 106, 12803. https://doi.org/10.1073/pnas.0905841106

Lovejoy, C., Massana, R., Pedrós-Alió, C., 2006. Diversity and Distribution of Marine Microbial Eukaryotes in the Arctic Ocean and Adjacent Seas. Appl. Environ. Microbiol. 72, 3085. https://doi.org/10.1128/AEM.72.5.3085-3095.2006

Mackinder, L.C.M., Worthy, C.A., Biggi, G., Hall, M., Ryan, K.P., Varsani, A., Harper, G.M., Wilson, W.H., Brownlee, C., Schroeder, D.C., 2009. A unicellular algal virus, Emiliania huxleyi virus 86, exploits an animal-like infection strategy. Journal of General Virology 90, 2306–2316. https://doi.org/10.1099/vir.0.011635-0

Marie, D., Brussaard, C.P.D., Thyrhaug, R., Bratbak, G., Vaulot, D., 1999. Enumeration of Marine Viruses in Culture and Natural Samples by Flow Cytometry. Appl. Environ. Microbiol. 65, 8. https://aem.asm.org/content/65/1/45.long

Martinez, J.M., Schroeder, D.C., Larsen, A., Bratbak, G., Wilson, W.H., 2007. Molecular Dynamics of *Emiliania huxleyi* and Cooccurring Viruses during Two Separate Mesocosm Studies. Applied and Environmental Microbiology 73, 554–562. https://doi.org/10.1128/AEM.00864-06

Martiny, J.B.H., Riemann, L., Marston, M.F., Middelboe, M., 2014. Antagonistic Coevolution of Marine Planktonic Viruses and Their Hosts. Annu. Rev. Mar. Sci. 6, 393–414. https://doi.org/10.1146/annurev-marine-010213-135108

Medlin, L.K., Barker, G.L.A., Campbell, L., Green, J.C., Hayes, P.K., Marie, D., Wrieden, S., Vaulot, D., 1996. Genetic characterisation of *Emiliania huxleyi* (Haptophyta). Journal of Marine Systems 9, 13–31. https://doi.org/10.1016/0924-7963(96)00013-9

Middelboe, M., Holmfeldt, K., Riemann, L., Nybroe, O., Haaber, J., 2009. Bacteriophages drive strain diversification in a marine Flavobacterium: implications for phage resistance and physiological properties. Environmental Microbiology 11, 1971–1982. https://doi.org/10.1111/j.1462-2920.2009.01920.x

Munn, C., 2011. Marine Microbiology - Ecology and Applications, 2nd ed. Garland Science, Taylor and Francis Group, LLC, New York and London.

Nagasaki, K., Ando, M., Itakura, S., Imai, I., Ishida, Y., 1994. Viral mortality in the final stage of *Heterosigma akashiwo* (Raphidophyceae) red tide. Journal of Plankton Research 16, 1595–1599. https://doi.org/10.1093/plankt/16.11.1595

Nagasaki, K., Tomaru, Y., Nakanishi, K., Hata, N., Katanozaka, N., Yamaguchi, M., 2004. Dynamics of *Heterocapsa circularisquama* (Dinophyceae) and its viruses in Ago Bay, Japan. Aquat. Microb. Ecol. 34, 219–226. https://doi.org/10.3354/ame034219

Nagasaki, K., Tomaru, Y., Tarutani, K., Katanozaka, N., Yamanaka, S., Tanabe, H., Yamaguchi, M., 2003. Growth Characteristics and Intraspecies Host Specificity of a Large Virus Infecting the Dinoflagellate *Heterocapsa circularisquama*. Appl. Environ. Microbiol. 69, 2580. https://doi.org/10.1128/AEM.69.5.2580-2586.2003

Nissimov, J.I., Napier, J.A., Allen, M.J., Kimmance, S.A., 2016. Intragenus competition between coccolithoviruses: an insight on how a select few can come to dominate many. Environmental Microbiology 18, 133–145. https://doi.org/10.1111/1462-2920.12902

Noble, R.T., Fuhrman, J.A., 1997. Virus decay and its causes in coastal waters. Appl. Environ. Microbiol. 63, 77. http://aem.asm.org/content/63/1/77.abstract

Paez-Espino, D., Eloe-Fadrosh, E.A., Pavlopoulos, G.A., Thomas, A.D., Huntemann, M., Mikhailova, N., Rubin, E., Ivanova, N.N., Kyrpides, N.C., 2016. Uncovering Earth's virome. Nature 536, 425. https://doi.org/10.1038/nature19094

Pagarete, A., Kusonmano, K., Petersen, K., Kimmance, S.A., Martínez Martínez, J., Wilson,

W.H., Hehemann, J.-H., Allen, M.J., Sandaa, R.-A., 2014. Dip in the gene pool: Metagenomic survey of natural coccolithovirus communities. Virology 466–467, 129–137. https://doi.org/10.1016/j.virol.2014.05.020

Peterson, B.W., Sharma, P.K., van der Mei, H.C., Busscher, H.J., 2012. Bacterial cell surface damage due to centrifugal compaction. Applied and environmental microbiology 78, 120–125. https://doi.org/10.1128/AEM.06780-11

Pommier, T., Canback, B., Riemann, L., Bostrom, K.H., SIMU, K., Lundberg, P., Tunlid, A., Hagstrom, Å., 2007. Global patterns of diversity and community structure in marine bacterioplankton. Molecular Ecology 16, 867–880. https://doi.org/10.1111/j.1365-294X.2006.03189.x

Proctor, L.M., Fuhrman, J.A., 1990. Viral mortality of marine bacteria and cyanobacteria. Nature 343, 60–62. https://doi.org/10.1038/343060a0

Refardt, D., Bergmiller, T., Kümmerli, R., 2013. Altruism can evolve when relatedness is low: evidence from bacteria committing suicide upon phage infection. Proceedings of the Royal Society B: Biological Sciences 280, 20123035. https://doi.org/10.1098/rspb.2012.3035

Rodrigues, M., Fan, J., Lyon, C., Wan, M., Hu, Y., 2018. Role of Extracellular Vesicles in Viral and Bacterial Infections: Pathogenesis, Diagnostics, and Therapeutics. Theranostics 8, 2709–2721. https://doi.org/10.7150/thno.20576

Rowe, J.M., Fabre, M.-F., Gobena, D., Wilson, W.H., Wilhelm, S.W., 2011. Application of the major capsid protein as a marker of the phylogenetic diversity of Emiliania huxleyi viruses: The major capsid protein of Emiliania huxleyi viruses. FEMS Microbiology Ecology 76, 373–380. https://doi.org/10.1111/j.1574-6941.2011.01055.x

Ruiz, E., Oosterhof, M., Sandaa, R.-A., Larsen, A., Pagarete, A., 2017. Emerging Interaction Patterns in the *Emiliania huxleyi*-EhV System. Viruses 9. https://doi.org/10.3390/v9030061

Sahlsten, E., 1998. Seasonal abundance in Skagerrak-Kattegat coastal waters and host specificity of viruses infecting the marine photosynthetic flagellate *Micromonas pusilla*. Aquat. Microb. Ecol. 16, 103–108. https://doi.org/10.3354/ame016103

Sandaa, R.-A., Heldal, M., Castberg, T., Thyrhaug, R., Bratbak, G., 2001. Isolation and Characterization of Two Viruses with Large Genome Size Infecting *Chrysochromulina ericina* (Prymnesiophyceae) and *Pyramimonas orientalis* (Prasinophyceae). Virology 290, 272–280. https://doi.org/10.1006/viro.2001.1161

Sandaa, R.-A., Storesund, J.E., Olesin, E., Paulsen, M.L., Larsen, A., Bratbak, G., Ray, J.L., 2018. Seasonality Drives Microbial Community Structure, Shaping both Eukaryotic and Prokaryotic Host–Viral Relationships in an Arctic Marine Ecosystem. Viruses **2018** 10, 715. https://doi.org/10.3390/v10120715

Schatz, D., Rosenwasser, S., Malitsky, S., Wolf, S.G., Feldmesser, E., Vardi, A., 2017. Communication via extracellular vesicles enhances viral infection of a cosmopolitan alga. Nature Microbiology 2, 1485–1492. https://doi.org/10.1038/s41564-017-0024-3

Schroeder, D.C., Oke, J., Hall, M., Malin, G., Wilson, W.H., 2003. Virus Succession Observed during an *Emiliania huxleyi* Bloom. Applied and Environmental Microbiology 69, 2484–2490. https://doi.org/10.1128/AEM.69.5.2484-2490.2003

Schroeder, D.C., Oke, J., Malin, G., Wilson, W.H., 2002. Coccolithovirus (Phycodnaviridae): Characterisation of a new large dsDNA algal virus that infects *Emiliana huxleyi*. Archives of Virology 147, 1685–1698. https://doi.org/10.1007/s00705-002-0841-3

Schwartz, D.C., Cantor, C.R., 1984. Separation of yeast chromosome-sized DNAs by pulsed field gradient gel electrophoresis. Cell 37, 67–75. https://doi.org/10.1016/0092-8674(84)90301-5

Sheldon, B.C., Verhulst, S., 1996. Ecological immunology: costly parasite defences and trade-offs in evolutionary ecology. Trends in Ecology & Evolution 11, 317–321. https://doi.org/10.1016/0169-5347(96)10039-2

Short, S.M., 2012. The ecology of viruses that infect eukaryotic algae: Algal virus ecology. Environmental Microbiology 14, 2253–2271. https://doi.org/10.1111/j.1462-2920.2012.02706.x

Shub, D.A., 1994. Bacterial Viruses: Bacterial altruism? Current Biology 4, 555–556. https://doi.org/10.1016/S0960-9822(00)00124-X

Soler, N., Marguet, E., Verbavatz, J.-M., Forterre, P., 2008. Virus-like vesicles and extracellular DNA produced by hyperthermophilic archaea of the order Thermococcales. Research in Microbiology 159, 390–399. https://doi.org/10.1016/j.resmic.2008.04.015

Sorensen, G., Baker, A.C., Hall, M.J., Munn, C.B., Schroeder, D.C., 2009. Novel virus dynamics in an *Emiliania huxleyi* bloom. Journal of Plankton Research 31, 787–791. https://doi.org/10.1093/plankt/fbp027

Suttle, C., Chan, A., 1993. Marine cyanophages infecting oceanic and coastal strains of Synechococcus: abundance, morphology, cross-infectivity and growth characteristics. Marine Ecology Progress Series 92, 99–109. https://doi.org/10.3354/meps092099

Suttle, C.A., 2007. Marine viruses — major players in the global ecosystem. Nature Reviews Microbiology 5, 801–812. https://doi.org/10.1038/nrmicro1750

Suttle, C.A., 2005. Viruses in the sea. Nature 437, 356–361. https://doi.org/10.1038/nature04160

Suttle, C.A., Chen, F., 1992. Mechanisms and Rates of Decay of Marine Viruses in Seawater. Appl. Environ. Microbiol. 58, 3721. http://aem.asm.org/content/58/11/3721.abstract

Szempruch, A.J., Dennison, L., Kieft, R., Harrington, J.M., Hajduk, S.L., 2016. Sending a message: extracellular vesicles of pathogenic protozoan parasites. Nature Reviews Microbiology 14, 669. https://doi.org/10.1038/nrmicro.2016.110

Tarutani, K., Nagasaki, K., Yamaguchi, M., 2000. Viral impacts on total abundance and clonal composition of the harmful bloom-forming phytoplankton *Heterosigma akashiwo*.

Appl Environ Microbiol 66, 4916–4920. https://doi.org/10.1128/aem.66.11.4916-4920.2000

Thingstad, T.F., 2000. Elements of a theory for the mechanisms controlling abundance, diversity, and biogeochemical role of lytic bacterial viruses in aquatic systems. Limnology and Oceanography 45, 1320–1328. https://doi.org/10.4319/lo.2000.45.6.1320

Thingstad, T.F., Våge, S., Storesund, J.E., Sandaa, R.-A., Giske, J., 2014. A theoretical analysis of how strain-specific viruses can control microbial species diversity. Proc. Natl. Acad. Sci. USA 111, 7813. https://doi.org/10.1073/pnas.1400909111

Thompson, J.D., Higgins, D.G., Gibson, T.J., 1994. CLUSTAL W: improving the sensitivity of progressive multiple sequence alignment through sequence weighting, position-specific gap penalties and weight matrix choice. Nucleic acids research 22, 4673–4680. https://www.ncbi.nlm.nih.gov/pubmed/7984417

Thompson, J.R., Pacocha, S., Pharino, C., Klepac-Ceraj, V., Hunt, D.E., Benoit, J., Sarma-Rupavtarm, R., Distel, D.L., Polz, M.F., 2005. Genotypic Diversity Within a Natural Coastal Bacterioplankton Population. Science 307, 1311. https://doi.org/10.1126/science.1106028

Tomaru, Y., Fujii, N., Oda, S., Toyoda, K., Nagasaki, K., 2011a. Dynamics of diatom viruses on the western coast of Japan. Aquat. Microb. Ecol. 63, 223–230. https://doi.org/10.3354/ame01496

Tomaru, Y., Shirai, Y., Toyoda, K., Nagasaki, K., 2011b. Isolation and Characterisation of a single-stranded DNA virus infecting the marine planktonic diatom *Chaetoceros tenuissimus*. Aquat. Microb. Ecol. 64, 175–184. https://doi.org/10.3354/ame01517

Tomaru, Y., Takao, Y., Suzuki, H., Nagumo, T., Koike, K., Nagasaki, K., 2011c. Isolation and Characterization of a Single-Stranded DNA Virus Infecting *Chaetoceros lorenzianus* Grunow. Appl. Environ. Microbiol. 77, 5285. https://doi.org/10.1128/AEM.00202-11

Tomaru, Y., Tarutani, K., Yamaguchi, M., Nagasaki, K., 2004. Quantitative and qualitative impacts of viral infection on a *Heterosigma akashiwo* (Raphidophyceae) bloom in Hiroshima Bay, Japan. Aquat. Microb. Ecol. 34, 227–238. https://doi.org/10.3354/ame034227

Tsuji, Y., Yoshida, M., 2017. Biology of Haptophytes: Complicated Cellular Processes Driving the Global Carbon Cycle, in: Advances in Botanical Research. Elsevier, pp. 219–261. https://doi.org/10.1016/bs.abr.2017.07.002

Tyrrell, T., Merico, A., 2004. *Emiliania huxleyi*: bloom observations and the conditions that induce them, in: Thierstein, H.R., Young, J.R. (Eds.), Coccolithophores: From Molecular Processes to Global Impact. Springer Berlin Heidelberg, Berlin, Heidelberg, pp. 75–97. https://doi.org/10.1007/978-3-662-06278-4_4

Våge, S., Pree, B., Thingstad, T.F., 2016. Linking internal and external bacterial community control gives mechanistic framework for pelagic virus-to-bacteria ratios. Environmental Microbiology 18, 3932–3948. https://doi.org/10.1111/1462-2920.13391

Van Etten, J.L., Burbank, D.E., Kuczmarski, D., Meints, R.H., 1983a. Virus Infection of Culturable Chlorella-Like Algae and Delevelopment of a Plaque Assay. Science 219, 994.

https://doi.org/10.1126/science.219.4587.994

Van Etten, J.L., Burbank, D.E., Xia, Y., Meints, R.H., 1983b. Growth cycle of a virus, PBCV-1, that infects Chlorella-like algae. Virology 126, 117–125. https://doi.org/10.1016/0042-6822(83)90466-X

Van Etten, J.L., Graves, M.V., Müller, D.G., Boland, W., Delaroque, N., 2002. Phycodnaviridae– large DNA algal viruses. Archives of Virology 147, 1479–1516. https://doi.org/10.1007/s00705-002-0822-6

Vardi, A., Van Mooy, B.A.S., Fredricks, H.F., Popendorf, K.J., Ossolinski, J.E., Haramaty, L., Bidle, K.D., 2009. Viral Glycosphingolipids Induce Lytic Infection and Cell Death in Marine Phytoplankton. Science 326, 861. https://doi.org/10.1126/science.1177322

Westbroek, P., Brown, C.W., Bleijswijk, J. van, Brownlee, C., Brummer, G.J., Conte, M., Egge, J., Fernández, E., Jordan, R., Knappertsbusch, M., Stefels, J., Veldhuis, M., van der Wal, P., Young, J., 1993. A model system approach to biological climate forcing. The example of *Emiliania huxleyi*. Global and Planetary Change 8, 27–46. https://doi.org/10.1016/0921-8181(93)90061-R

Wilhelm, S.W., Suttle, C.A., 1999. Viruses and Nutrient Cycles in the Sea. BioScience 49, 781–788. https://doi.org/10.2307/1313569

Wilson, W.H., Carr, N.G., Mann, N.H., 1996. The effect of phosphate status on the kinetics of cyanophage infection in the oceanic cyanobacterium synechococcus sp. WH78031. Journal of Phycology 32, 506–516. https://doi.org/10.1111/j.0022-3646.1996.00506.x

Wilson, W.H., Schroeder, D.C., Allen, M.J., Holden, M.T.G., Parkhill, J., Barrell, B.G., Churcher, C., Hamlin, N., Mungall, K., Norbertczak, H., Quail, M.A., Price, C., Rabbinowitsch, E., Walker, D., Craigon, M., Roy, D., Ghazal, P., 2005. Complete Genome Sequence and Lytic Phase Transcription Profile of a Coccolithovirus. Science 309, 1090. https://doi.org/10.1126/science.1113109

Wilson, W.H., Tarran, G.A., Schroeder, D., Cox, M., Oke, J., Malin, G., 2002. Isolation of viruses responsible for the demise of an *Emiliania huxleyi* bloom in the English Channel. Journal of the Marine Biological Association of the United Kingdom 82, 369–377. https://doi.org/10.1017/S002531540200560X

Wilson, W.H., Van Etten, J.L., Allen, M.J., 2009. The Phycodnaviridae: The Story of How Tiny Giants Rule the World, in: Van Etten, J.L. (Ed.), Lesser Known Large DsDNA Viruses. Springer Berlin Heidelberg, Berlin, Heidelberg, pp. 1–42. https://doi.org/10.1007/978-3-540-68618-7_1

Wilson, W.H., Van Etten, J.L., Schroeder, D.C., Nagasaki, K., Brussaard, C.P.D., Bratbak, G., Suttle, C.A., 2011. Phycodnaviridae - dsDNA Viruses, ICTV 9th report [WWW Document]. International Committee on Taxonomy of Viruses (ICTV). https://talk.ictvonline.org/ictv-reports/ictv_9th_report/dsdna-viruses-2011/w/dsdna_viruses/123/phycodnaviridae (accessed 4.10.19).

Winter, A., Siesser, W.G., 2006. Coccolithophores. Cambridge University Press.

Winter, C., Bouvier, T., Weinbauer, M.G., Thingstad, T.F., 2010. Trade-offs between competition and defense specialists among unicellular planktonic organisms: the “killing the winner” hypothesis revisited. Microbiol Mol Biol Rev 74, 42–57. https://doi.org/10.1128/MMBR.00034-09

Wommack, K.E., Colwell, R.R., 2000. Virioplankton: Viruses in Aquatic Ecosystems. Microbiology and Molecular Biology Reviews 64, 69–114. https://doi.org/10.1128/MMBR.64.1.69-114.2000

Yáñez-Mó, M., Siljander, P.R.-M., Andreu, Z., Bedina Zavec, A., Borràs, F.E., Buzas, E.I., Buzas, K., Casal, E., Cappello, F., Carvalho, J., Colás, E., Cordeiro-da Silva, A., Fais, S., Falcon-Perez, J.M., Ghobrial, I.M., Giebel, B., Gimona, M., Graner, M., Gursel, I., Gursel, M., Heegaard, N.H.H., Hendrix, A., Kierulf, P., Kokubun, K., Kosanovic, M., Kralj-Iglic, V., Krämer-Albers, E.-M., Laitinen, S., Lässer, C., Lener, T., Ligeti, E., Linē, A., Lipps, G., Llorente, A., Lötvall, J., Manček-Keber, M., Marcilla, A., Mittelbrunn, M., Nazarenko, I., Nolte-‘t Hoen, E.N.M., Nyman, T.A., O’Driscoll, L., Olivan, M., Oliveira, C., Pállinger, É., del Portillo, H.A., Reventós, J., Rigau, M., Rohde, E., Sammar, M., Sánchez-Madrid, F., Santarém, N., Schallmoser, K., Stampe Ostenfeld, M., Stoorvogel, W., Stukelj, R., Van der Grein, S.G., Helena Vasconcelos, M., Wauben, M.H.M., De Wever, O., 2015. Biological properties of extracellular vesicles and their physiological functions. Journal of Extracellular Vesicles 4, 27066. https://doi.org/10.3402/jev.v4.27066

Young, J.R., Westbroek, P., 1991. Genotypic variation in the coccolithophorid species *Emiliania huxleyi*. Marine Micropaleontology 18, 5–23. https://doi.org/10.1016/0377-8398(91)90004-P

Zipper, H., Brunner, H., Bernhagen, J., Vitzthum, F., 2004. Investigations on DNA intercalation and surface binding by SYBR Green I, its structure determination and methodological implications. Nucleic acids research 32, e103. https://doi.org/10.1093/nar/gnh101

Appendix A: Host and virus

Table A-1. *E. huxleyi* strain information

Strain	Isolation Site	Coordinates (Lat Long approximate)	Isolation date
CCMP374	North Atlantic Ocean	42.5° N 69° W	1990
CCMP371	North Atlantic Ocean	32° N 62° W	1987
B	Raunefjorden, Norway	60.2° N 5.2° E	1991

Table A-2. EhV strain information

Viral isolate	Isolation site	Isolation date	Coordinates (Lat long approximate)	Host Strain Used for Viral Propagation
EhV-86	English Channel	1999	50.15° N 4.13° W	CCMP374
EhV-208	English Channel	2001	50.15° N 4.13° W	CCMP374
EhV-99B1	Raunefjorden, Norway	1999	60.2° N 5.2° E	CCMP374

Appendix B: Protocols

B.1 Medium content

Table B-1. IMR/2 medium in 1L 70% seawater

Component	Containing	Stock solution	Quantity pr. L
KH_2PO_4		0.68 g / 100 mL dH_2O	500 µL
KNO_3		5 g / 100 mL dH_2O	500 µL
Trace metal solution	Na_2-EDTA (3g) NaFe-EDTA (800mg) $MnSO_4$ $4H_2O$ (410mg) $ZnSO_4$ $7H_2O$ (125mg) Na_2MoO_4 $2H_2O$ (65mg) dH_2O (500mL) $CuSO_4/CoCl_2$-solution (0.5mL) - $CuSO_4$ $5H_2O$ (0.4g) - $CoCl_2$ $6H_2O$ (0.4g) - dH_2O (100mL)		500 µL
Vitamin solution	Thiamin (vit. B) (50mg) Biotin (0.5mg) B_{12}-solution (0.5mL) - 100mg B_{12}/100mL dH_2O dH_2O (500mL)		500 µL
Selenium (Na_2SeO_3)		2mg/100mL dH_2O	250 µL

Table B-2. f/2 medium in 1L 70% seawater

Component	Containing	Stock Solution	Quantity pr. L
$NaNO_3$		7.5g/100mL dH_2O	1 mL
NaH_2PO_4 H_2O		0.5g/100mL dH_2O	1 mL
Na_2SiO_3 $9H_2O$		3.0g/100mL dH_2O	1 mL
Trace metal solution (1L stock solution)	$FeCl_3$ $6H_2O$ (3.15g) Na_2EDTA $2H_2O$ (4.36g) $CuSO_4$ $5H_2O$ (1mL, 0.98g/100mL dH_2O) Na_2MoO_4 $2H_2O$ (1mL, 0.63g/100mL dH_2O) $ZnSO_4$ $7H_2O$ (1mL, 2.20g/100mL dH_2O) $CoCl_2$ $6H_2O$ (1mL, 1g/100mL dH_2O) $MnCl_2$ $4H_2O$ (1mL, 18g/100mL dH_2O)		1 mL
Vitamin solution (1 L stock solution)	Thiamin HCl (vit. B_1) (200mg) Biotin (vit. H) (0.1mg/mL dH_2O) Cyanocobalamin (vit. B_{12}) (1.0 mg/mL dH_2O)		0.5 mL

B.2 0.5 M EDTA (pH 8.0)

186.1 g of disodium EDTA (Na_2EDTA)
800 mL of dH_2O
Adjust the pH to 8.0 with NaOH (~50mL of NaOH)
Bring volume to 1 L with dH_2O
Stirr vigorously on a magnetic stirrer*
Sterilize by autoclaving
Store at room temperature

*The disodium salt of EDTA will not dissolve until the pH of the solution is adjusted to 8.0 by the addition of NaOH.

B.3 LA with 100µg/mL Ampicillin

10 g Tryptone
5 g Yeast extract
5 g NaCl
15 g Agar (skip this step for LB-medium)
1L dist. H_2O
Autoclave
Water bath at 60°C for approx. 30 min.

1 mL sterile filtered ampicillin solution (See below, LA-medium only)
Pour into petri-dishes

200 mg Ampicillin sodium salt
2 mL sterile dist. H_2O
Sterile filter at 0.2 µm syringe-filter (Schleicher & S. -røde)

Appendix C: Results

C.1 Gel Electrophoresis

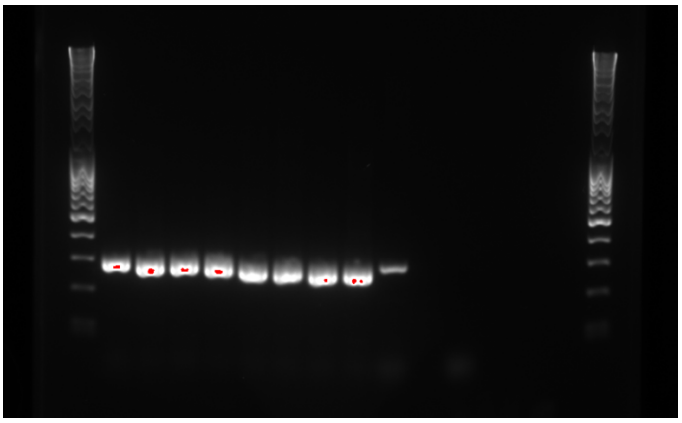

Figure C-1. Image example of *mcp* amplicons from PCR product, run on a 1.5% agarose gel with a MassRuler ladder. The nine bands represent presence of *mcp* gene from the PCR products and the last band is a positive control. Negative control was added next to positive control with an empty well in between.

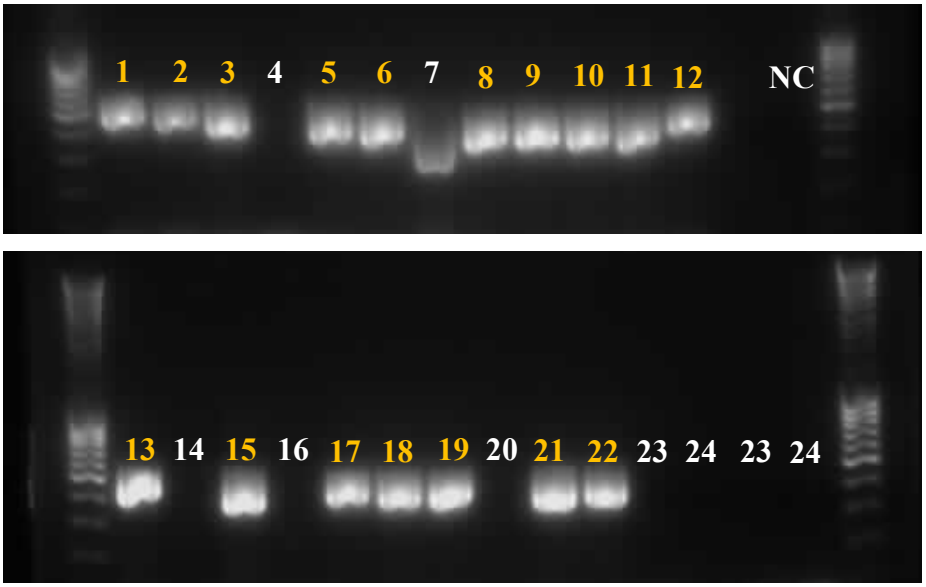

Figure C-2. Image of cloned *mcp* regions run on a 1.5% agarose gel with a MassRuler ladder. There were six PCR-products from each of the four isolates (added chronologically) and the bands suggest presence of cloned *mcp*. Bands 1-6 is isolate MRH9, 7-12 is MRB9, 13-18 is MRC9 and 19-24 is MRG11. NC represents negative control. Numbers marked with orange represents samples used further in the cloning process.

C.2 Flow Cytometry gating in cross-infection experiment

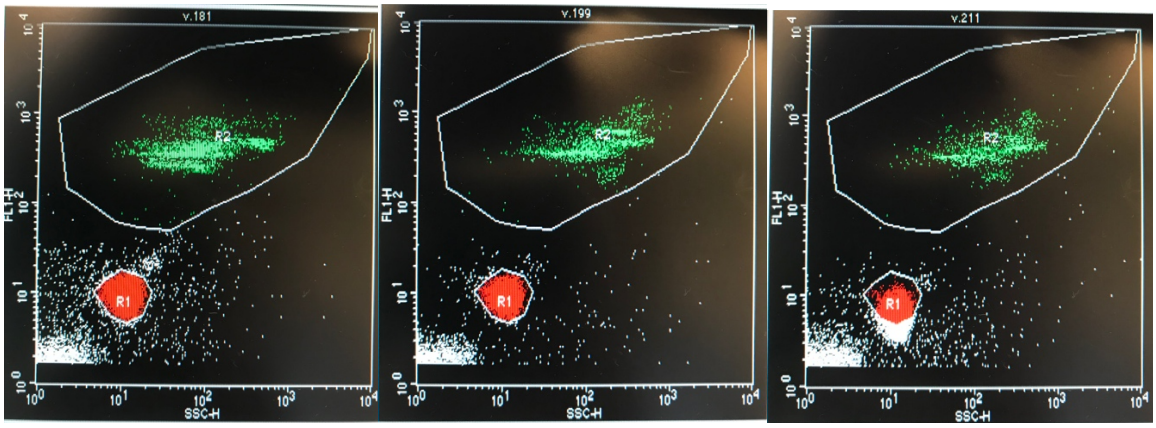

Figure C-3. Flow cytometry gating with fixed and stained samples from three days post infection of EhV-99B1 with side scatter (SSC) and fluorescence (FL) on x and y-axis, respectively. The viral population of infected culture of CCMP374, CCMP371 and B is represented in the three graphs (left to right). Gates R1 (red) and R2 (green) represents EhV and bacterial population, respectively.

C.3 Average in situ relative fluorescence on MPN plates

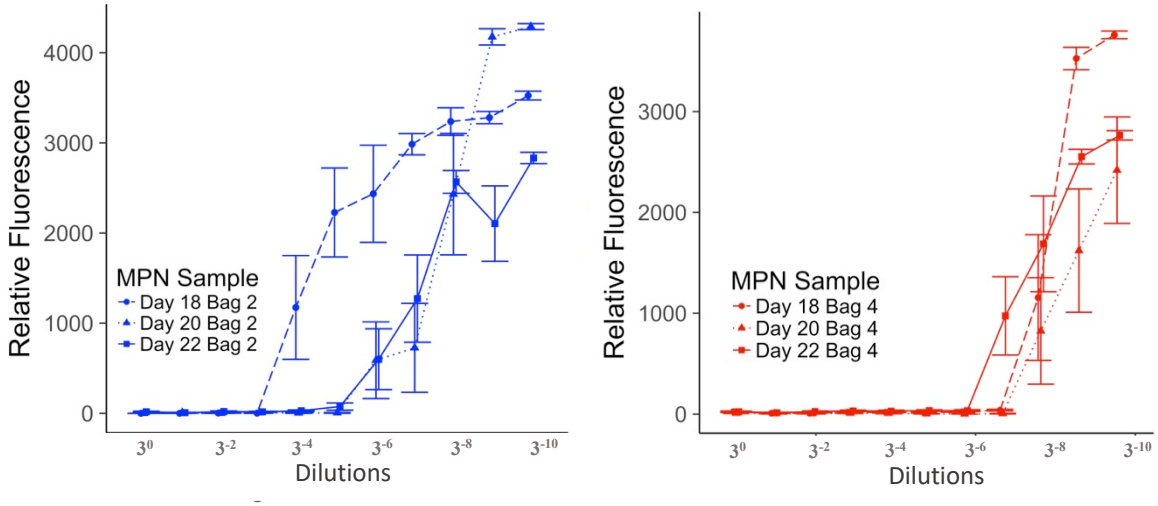

Figure C-4. Graphs represent the average *in situ* relative fluorescence for susceptible host strain CCMP374 on MPN plates added filtered sample water from mesocosm bags 2 (in blue) and 4 (in red) from day 18 (circular points, solid lines), 20 (triangular points, dotted lines) and 22 (squared points, dashed lines). Each value on the x-axis represent the average relative fluorescence of all eight wells in a column of the MPN plates with standard error bar. The data points have been dodged (x-axis) in order to separate them where there is overlap.

C.4 Sequences Mesocosm isolates

Alignment C-1. CLUSTAL 2.1 multiple sequence alignment of isolated EhV

```
MCP_MRB9_D20_Bag2_MR11       -CGAAGAACGCCTCGGTGTACGCACCCTCAATGTATGGAAGGACGTGCGA
MCP_MRC9_D22_Bag4_MR17       -CGATGAACGCCTCGGTGTACGCACCCTCAATGTATGGAAGGACGTGCGA
MCP_MRH9_D22_Bag2_MR06       -CGCGCCACGCCTCGGTGTACGCACCCTCAATGTATGGAAGGACGTGCGA
MCP_MRC9_D22_Bag4_MR15       -CGGCCAACGCCTCGGTGTACGCACCCTCAATGTATGGAAGGACGTGCGA
MCP_MRB9_D20_Bag2_MR10       GTACCAA-CGCCTCGGTGTACGCACCCTCAATGTATGGAAGGACGTGCGA
MCP_MRB9_D20_Bag2_MR12       -TACCAAACGCCTCGGTGTACGCACCCTCAATGTATGGAAGGACGTGCGA
MCP_MRH9_D22_Bag2_MR01       -GTTTGGACGCCTCGGTGTACGCACCCTCAATGTATGGAAGGACGTGCGA
MCP_MRH9_D22_Bag2_MR05       -GTTTGGACGCCTCGGTGTACGCACCCTCAATGTATGGAAGGACGTGCGA
MCP_MRH9_D22_Bag2_MR03       -CACAGGACGCCTCGGTGTACGCACCCTCAATGTATGGAAGGACGTGCGA
MCP_MRG11_D20_Bag4_MR21      -AAAAGGACGCCTCGGTGTACGCACCCTCAATGTATGGAAGGACGTGCGA
MCP_MRH9_D22_Bag2_MR02       -------ACGCCTCGGTGTACGCACCCTCAATGTATGGAAGGACGTGCGA
MCP_MRB9_D20_Bag2_MR08       -GGATGTACGCCTCGGTGTACGCACCCTCAATGTATGGAAGGACGTGCGA
MCP_MRB9_D20_Bag2_MR09       -GGGGGGACGCCTCGGTGTACGCACCCTCAATGTATGGAAGGACGTGCGA
MCP_MRC9_D22_Bag4_MR13       -GGTGCCACGCCTCGGTGTACGCACCCTCAATGTATGGAAGGACGTGCGA
MCP_MRG11_D20_Bag4_MR22      -GGGGGCACGCCTCGGTGTACGCACCCTCAATGTATGGAAGGACGTGCGA
MCP_MRC9_D22_Bag4_MR18       -GCAAAAACGCCTCGGTGTACGCACCCTCAATGTATGGAAGGACGTGCGA
                                      ****************************************

MCP_MRB9_D20_Bag2_MR11       TACATCAGCCTGCGCAGCGACGTCGTTGTCGAGCGACGCGAACGACTGCT
MCP_MRC9_D22_Bag4_MR17       TACATCAGCCTGCGCAGCGACGTCGTTGTCGAGCGACGCGAACGACTGCT
MCP_MRH9_D22_Bag2_MR06       TACATCAGCCTGCGCAGCGACGTCGTTGTCGAGCGACGCGAACGACTGCT
MCP_MRC9_D22_Bag4_MR15       TACATCAGCCTGCGCAGCGACGTCGTTGTCGAGCGACGCGAACGACTGCT
MCP_MRB9_D20_Bag2_MR10       TACATCAGCCTGCGCAGCGACGTCGTTGTCGAGCGACGCGAACGACTGCT
MCP_MRB9_D20_Bag2_MR12       TACATCAGCCTGCGCAGCGACGTCGTTGTCGAGCGACGCGAACGACTGCT
MCP_MRH9_D22_Bag2_MR01       TACATCAGCCTGCGCAGCGACGTCGTTGTCGAGCGACGCGAACGACTGCT
MCP_MRH9_D22_Bag2_MR05       TACATCAGCCTGCGCAGCGACGTCGTTGTCGAGCGACGCGAACGACTGCT
MCP_MRH9_D22_Bag2_MR03       TACATCAGCCTGCGCAGCGACGTCGTTGTCGAGCGACGCGAACGACTGCT
MCP_MRG11_D20_Bag4_MR21      TACATCAGCCTGCGCAGCGACGTCGTTGTCGAGCGACGCGAACGACTGCT
MCP_MRH9_D22_Bag2_MR02       TACATCAGCCTGCGCAGCGACGTCGTTGTCGAGCGACGCGAACGACTGCT
MCP_MRB9_D20_Bag2_MR08       TACATCAGCCTGCGCAGCGACGTCGTTGTCGAGCGACGCGAACGACTGCT
MCP_MRB9_D20_Bag2_MR09       TACATCAGCCTGCGCAGCGACGTCGTTGTCGAGCGACGCGAACGACTGCT
MCP_MRC9_D22_Bag4_MR13       TACATCAGCCTGCGCAGCGACGTCGTTGTCGAGCGACGCGAACGACTGCT
MCP_MRG11_D20_Bag4_MR22      TACATCAGCCTGCGCAGCGACGTCGTTGTCGAGCGACGCGAACGACTGCT
MCP_MRC9_D22_Bag4_MR18       TACATCAGCCTGCGCAGCGACGTCGTTGTCGAGCGACGCGAACGACTGCT
                             ************************************************

MCP_MRB9_D20_Bag2_MR11       GAGTTGGCTGAACGGTGTCCGCCTGGTTCTGGACCTTTAGGCCAGGGAGG
MCP_MRC9_D22_Bag4_MR17       GAGTTGGCTGAACGGTGTCCGCCTGGTTCTGGACCTTTAGGCCAGGGAGG
MCP_MRH9_D22_Bag2_MR06       GAGTTGGCTGAACGGTGTCCGCCTGGTTCTGGACCTTTAGGCCAGGGAGG
MCP_MRC9_D22_Bag4_MR15       GAGTTGGCTGAACGGTGTCCGCCTGGTTCTGGACCTTTAGGCCAGGGAGG
MCP_MRB9_D20_Bag2_MR10       GAGTTGGCTGAACGGTGTCCGCCTGGTTCTGGACCTTTAGGCCAGGGAGG
MCP_MRB9_D20_Bag2_MR12       GAGTTGGCTGAACGGTGTCCGCCTGGTTCTGGACCTTTAGGCCAGGGAGG
MCP_MRH9_D22_Bag2_MR01       GAGTTGGCTGAACGGTGTCCGCCTGGTTCTGGACCTTTAGGCCAGGGAGG
MCP_MRH9_D22_Bag2_MR05       GAGTTGGCTGAACGGTGTCCGCCTGGTTCTGGACCTTTAGGCCAGGGAGG
MCP_MRH9_D22_Bag2_MR03       GAGTTGGCTGAACGGTGTCCGCCTGGTTCTGGACCTTTAGGCCAGGGAGG
MCP_MRG11_D20_Bag4_MR21      GAGTTGGCTGAACGGTGTCCGCCTGGTTCTGGACCTTTAGGCCAGGGAGG
MCP_MRH9_D22_Bag2_MR02       GAGTTGGCTGAACGGTGTCCGCCTGGTTCTGGACCTTTAGGCCAGGGAGG
MCP_MRB9_D20_Bag2_MR08       GAGTTGGCTGAACGGTGTCCGCCTGGTTCTGGACCTTTAGGCCAGGGAGG
MCP_MRB9_D20_Bag2_MR09       GAGTTGGCTGAACGGTGTCCGCCTGGTTCTGGACCTTTAGGCCAGGGAGG
MCP_MRC9_D22_Bag4_MR13       GAGTTGGCTGAACGGTGTCCGCCTGGTTCTGGACCTTTAGGCCAGGGAGG
MCP_MRG11_D20_Bag4_MR22      GAGTTGGCTGAACGGTGTCCGCCTGGTTCTGGACCTTTAGGCCAGGGAGG
MCP_MRC9_D22_Bag4_MR18       GAGTTGGCTGAACGGTGTCCGCCTGGTTCTGGACCTTTAGGCCAGGGAGG
                             ************************************************
```

```
MCP_MRB9_D20_Bag2_MR11      ACAATCTTGAGGTACATCCACGAAAGAAGGTCGCCTTGCCTATTGACGGT
MCP_MRC9_D22_Bag4_MR17      ACAATCTTGAGGTACATCCACGAAAGAAGGTCGCCTTGCCTATTGACGGT
MCP_MRH9_D22_Bag2_MR06      ACAATCTTGAGGTACATCCACGAAAGAAGGTCGCCTTGCCTATTGACGGT
MCP_MRC9_D22_Bag4_MR15      ACAATCTTGAGGTACATCCACGAAAGAAGGTCGCCTTGCCTATTGACGGT
MCP_MRB9_D20_Bag2_MR10      ACAATCTTGAGGTACATCCACGAAAGAAGGTCGCCTTGCCTATTGACGGT
MCP_MRB9_D20_Bag2_MR12      ACAATCTTGAGGTACATCCACGAAAGAAGGTCGCCTTGCCTATTGACGGT
MCP_MRH9_D22_Bag2_MR01      ACAATCTTGAGGTACATCCACGAAAGAAGGTCGCCTTGCCTATTGACGGT
MCP_MRH9_D22_Bag2_MR05      ACAATCTTGAGGTACATCCACGAAAGAAGGTCGCCTTGCCTATTGACGGT
MCP_MRH9_D22_Bag2_MR03      ACAATCTTGAGGTACATCCACGAAAGAAGGTCGCCTTGCCTATTGACGGT
MCP_MRG11_D20_Bag4_MR21     ACAATCTTGAGGTACATCCACGAAAGAAGGTCGCCTTGCCTATTGACGGT
MCP_MRH9_D22_Bag2_MR02      ACAATCTTGAGGTACATCCACGAAAGAAGGTCGCCTTGCCTATTGACGGT
MCP_MRB9_D20_Bag2_MR08      ACAATCTTGAGGTACATCCACGAAAGAAGGTCGCCTTGCCTATTGACGGT
MCP_MRB9_D20_Bag2_MR09      ACAATCTTGAGGTACATCCACGAAAGAAGGTCGCCTTGCCTATTGACGGT
MCP_MRC9_D22_Bag4_MR13      ACAATCTTGAGGTACATCCACGAAAGAAGGTCGCCTTGCCTATTGACGGT
MCP_MRG11_D20_Bag4_MR22     ACAATCTTGAGGTACATCCACGAAAGAAGGTCGCCTTGCCTATTGACGGT
MCP_MRC9_D22_Bag4_MR18      ACAATCTTGAGGTACATCCACGAAAGAAGGTCGCCTTGCCTATTGACGGT
                            **************************************************

MCP_MRB9_D20_Bag2_MR11      AATATGCGACTCAGCCCCAAACTGAACCTGGGTTGTGAATGGCTGATTGA
MCP_MRC9_D22_Bag4_MR17      AATATGCGACTCAGCCCCAAACTGAACCTGGGTTGTGAATGGCTGATTGA
MCP_MRH9_D22_Bag2_MR06      AATATGCGACTCAGCCCCAAACTGAACCTGGGTTGTGAATGGCTGATTGA
MCP_MRC9_D22_Bag4_MR15      AATATGCGACTCAGCCCCAAACTGAACCTGGGTTGTGAATGGCTGATTGA
MCP_MRB9_D20_Bag2_MR10      AATATGCGACTCAGCCCCAAACTGAACCTGGGTTGTGAATGGCTGATTGA
MCP_MRB9_D20_Bag2_MR12      AATATGCGACTCAGCCCCAAACTGAACCTGGGTTGTGAATGGCTGATTGA
MCP_MRH9_D22_Bag2_MR01      AATATGCGACTCAGCCCCAAACTGAACCTGGGTTGTGAATGGCTGATTGA
MCP_MRH9_D22_Bag2_MR05      AATATGCGACTCAGCCCCAAACTGAACCTGGGTTGTGAATGGCTGATTGA
MCP_MRH9_D22_Bag2_MR03      AATATGCGACTCAGCCCCAAACTGAACCTGGGTTGTGAATGGCTGATTGA
MCP_MRG11_D20_Bag4_MR21     AATATGCGACTCAGCCCCAAACTGAACCTGGGTTGTGAATGGCTGATTGA
MCP_MRH9_D22_Bag2_MR02      AATATGCGACTCAGCCCCAAACTGAACCTGGGTTGTGAATGGCTGATTGA
MCP_MRB9_D20_Bag2_MR08      AATATGCGACTCAGCCCCAAACTGAACCTGGGTTGTGAATGGCTGATTGA
MCP_MRB9_D20_Bag2_MR09      AATATGCGACTCAGCCCCAAACTGAACCTGGGTTGTGAATGGCTGATTGA
MCP_MRC9_D22_Bag4_MR13      AATATGCGACTCAGCCCCAAACTGAACCTGGGTTGTGAATGGCTGATTGA
MCP_MRG11_D20_Bag4_MR22     AATATGCGACTCAGCCCCAAACTGAACCTGGGTTGTGAATGGCTGATTGA
MCP_MRC9_D22_Bag4_MR18      AATATGCGACTCAGCCCCAAACTGAACCTGGGTTGTGAATGGCTGATTGA
                            **************************************************

MCP_MRB9_D20_Bag2_MR11      TCGACTCGAGCGCGAAAAGCGAGTGCTTCTGGTACGAAGACTAGCTC
MCP_MRC9_D22_Bag4_MR17      TCGACTCGAGCGCGAAAAGCGAGTGCTTCTGGTACGAAGAC------
MCP_MRH9_D22_Bag2_MR06      TCGACTCGAGCGCGAAAAGCGAGTGCTTCTGGTACGAAGACAAGGTG
MCP_MRC9_D22_Bag4_MR15      TCGACTCGAGCGCGAAAAGCGAGTGCTTCTGGTACGAAGACTAGCAC
MCP_MRB9_D20_Bag2_MR10      TCGACTCGAGCGCGAAAAGCGAGTGCTTCTGGTACGAAGACCGGGCG
MCP_MRB9_D20_Bag2_MR12      TCGACTCGAGCGCGAAAAGCGAGTGCTTCTGGTACGAAGACGAAAAG
MCP_MRH9_D22_Bag2_MR01      TCGACTCGAGCGCGAAAAGCGAGTGCTTCTGGTACGAAGACCGAAGA
MCP_MRH9_D22_Bag2_MR05      TCGACTCGAGCGCGAAAAGCGAGTGCTTCTGGTACGAAGACCGAAGA
MCP_MRH9_D22_Bag2_MR03      TCGACTCGAGCGCGAAAAGCGAGTGCTTCTGGTACGAAGACAAAGTA
MCP_MRG11_D20_Bag4_MR21     TCGACTCGAGCGCGAAAAGCGAGTGCTTCTGGTACGAAGACACAACC
MCP_MRH9_D22_Bag2_MR02      TCGACTCGAGCGCGAAAAGCGAGTGCTTCTGGTACGAAGACATACCG
MCP_MRB9_D20_Bag2_MR08      TCGACTCGAGCGCGAAAAGCGAGTGCTTCTGGTACGAAGACCCGTCC
MCP_MRB9_D20_Bag2_MR09      TCGACTCGAGCGCGAAAAGCGAGTGCTTCTGGTACGAAGACAAGTCG
MCP_MRC9_D22_Bag4_MR13      TCGACTCGAGCGCGAAAAGCGAGTGCTTCTGGTACGAAGACTCGATT
MCP_MRG11_D20_Bag4_MR22     TCGACTCGAGCGCGAAAAGCGAGTGCTTCTGGTACGAAGACGGCGCG
MCP_MRC9_D22_Bag4_MR18      TCGACTCGAGCGCGAAAAGCGAGTGCTTCTGGTACGAAGACTGTTTT
                            ****************************************
```

C.5 OTUs Mesocosm

Table C-1. The most dominating EhV OTUs during the mesocosm in the two mesocosm bags and samples collected from the most dilute well of the MPN plate that resulted in lysis. The values represent number of hits.

Bag	Population	OTU1	OTU2	OTU3	OTU4	OTU5	OTU6	OTU7
Bag 2	D16	56790	121	219	0	0	0	0
Bag 2	D20	23319	50	167	0	394	0	0
Bag 2	D22	71042	182	272	0	0	0	0
Bag 4	D12	35966	90	182	0	0	0	0
Bag 4	D16	8121	0	0	0	0	0	0
Bag 4	D20	90713	141	230	107	1193	91	0
Bag 4	D22	127432	403	0	160	0	132	249
Bag 2	MPN D16	312266	1098	0	282	0	275	428
Bag 2	MPN D20	73799	217	0	129	0	0	101
Bag 2	MPN D22	63129	142	0	124	770	0	0
Bag 4	MPN D12	36388	92	0	93	578	0	0
Bag 4	MPN D16	298712	1000	0	310	0	312	411
Bag 4	MPN D20	68200	114	0	108	760	0	0
Bag 4	MPN D22	0	0	0	0	0	0	0

Alignment C-2. CLUSTAL 2.1 multiple sequence alignment of dominating OTUs and isolated EhV

```
OTU_Isolated_EhV      AATGTATGGAAGGACGTGCGATACATCAGCCTGCGCAGCGACGTCGTTGTCGAGCGACGC
OTU1                  AATGTATGGAAGGACGTGCGATACATCAGCCTGCGCAGCGACGTCGTTGTCGAGCGACGC
OTU3                  AATGTATGGAAGGACGTGCGATACATCAGCCTGCGCAGCGACGTCGTTGTCGAGCGCCGC
OTU4                  AATGTATGGAAGGACGTGCGATACATCAGCCTGCGCAGCGACGTCGTTGTCGAGCGACGC
OTU2                  AATGTATGGAAGGACGTGCGATACATCAGCCTGCGCAGCGACGTCGTTGTCGAGCGACGC
OTU5                  AATGTATGGAAGGACGTGCGATACATCAGCCTGCGCAGCGACGTCGTTGTCGAGCGACGC
                      ************************************************** ***

OTU_Isolated_EhV      GAACGACTGCTGAGTTGGCTGAACGGTGTCCGCCTGGTTCTGGACCTTTAGGCCAGGGAG
OTU1                  GAACGACTGCTGAGTTGGCTGAACGGTGTCCGCCTGGTTCTGGACCTTTAGGCCAGGGAG
OTU3                  GAACGACTGCTGAGTTGGCTGAACGGTGTCCGCCTGGTTCTGGACCTTTAGGCCAGGGAG
OTU4                  GAACGACTGCTGAGTTGGCTGAACGGTGTCCGCCTGGTTCTGGACCTTTAGGCCAGGGAG
OTU2                  GAACGACTGCTGAGTTGGCTGAACGGTGTCCGCCTGGTTCTGGACCTTTAGGCCAGGGAG
OTU5                  GAACGACTGCTGAGTTGGCTGAACGGTGTCCGCCTGGTTCTGGACCTTTAGGCCAGGGAG
                      ************************************************************

OTU_Isolated_EhV      GACAATCTTGAGGTACATCCACGAAAGAAGGTCGCCTTGCCTATTGACGGTAATATGCGA
OTU1                  GACAATCTTGAGGTACATCCACGAAAGAAGGTCGCCTTGCCTATTGACGGTAATATGCGA
OTU3                  GACAATCTTGAGGTACATCCACGAAAGAAGGTCGCCTTGCCTATTGACGGTAATATGCGA
OTU4                  GACAATCTTGAGGTACATCCACGAAAGAAGGTCGCCTTGCCTATTGACGGTAATATGTGA
OTU2                  GACAATCTTGAGGTACATCCACGAAAGAAGGTCGCCTTGCCTATTGACGGTAATATGCGA
OTU5                  GACAATCTTGAGGTACATCCACGAAAGAAGGTCGCCTTGCCTATTGACGGTAATATGCGA
                      ********************************************************** **

OTU_Isolated_EhV      CTCAGCCCCAAACTGAACCTGGGTTGTGAATGGCTGATTGATCGACTCGAGCGCGAAAA
OTU1                  CTCAGCCCCAAACTGAACCTGGGTTGTGAATGGCTGATTGATCGACTCGAGCGCGAAAA
OTU3                  CTCAGCCCCAAACTGAACCTGGGTTGTGAATGGCTGATTGATCGACTCGAGCGCGAAAA
OTU4                  CTCAGCCCCAAACTGAACCTGGGTTGTGAATGGCTGATTGATCGACTCGAGCGCGAAAA
OTU2                  CTCAGCCCCAAACTGAACCTGGGTTGTGAATGGCCGATTGATCGACTCGAGCGCGAAAA
OTU5                  CTCAGCCCCAAACTGAACCTGGGTTGTGAATGGCAGATTGATCGACTCGAGCGCGAAAA
                      ********************************** ************************
```